

Nonlinear Symmetry-Fragmentation of Nonabelian Anyons In Symmetry-Enriched Topological Phases: A String-Net Model Realization

Nianrui Fu^a Siyuan Wang^a Yu Zhao^{1a} Yidun Wan^{2a,b}

^a*State Key Laboratory of Surface Physics, Department of Physics, Center for Field Theory and Particle Physics, and Institute for Nanoelectronic devices and Quantum computing, Fudan University, Shanghai 200433, China*

^b*Hefei National Laboratory, Hefei 230088, China*

E-mail: nrfu21@m.fudan.edu.cn, siyuanwang18@fudan.edu.cn,
yuzhao20@fudan.edu.cn, ydwan@fudan.edu.cn

ABSTRACT: Symmetry-enriched topological (SET) phases combine intrinsic topological order with global symmetries, giving rise to novel symmetry phenomena. While SET phases with Abelian anyons are relatively well understood, those involving non-Abelian anyons remain elusive. This obscurity stems from the multi-dimensional internal gauge spaces intrinsic to non-Abelian anyons—a feature first made explicit in [1, 2] and further explored and formalized in our recent works [3–8]. These internal spaces can transform in highly nontrivial ways under global symmetries. In this work, we employ an exactly solvable model—the multifusion Hu-Geer-Wu string-net model introduced in a companion paper [9]—to reveal how the internal gauge spaces of non-Abelian anyons transform under symmetries. We uncover a universal mechanism, global symmetry fragmentation (GSF), whereby symmetry-invariant anyons exhibit internal Hilbert space decompositions into eigensubspaces labeled by generally fractional symmetry charges. Meanwhile, symmetry-permuted anyons hybridize and fragment their internal spaces in accordance with their symmetry behavior. These fragmented structures realize genuinely nonlinear symmetry representations—to be termed coherent representations—that transcend conventional linear and projective classifications, reflecting the categorical nature of symmetries in topological phases. Our results identify nonlinear fragmentation as a hallmark of non-Abelian SETs and suggest new routes for symmetry-enabled control in topological quantum computation.

¹Corresponding author

²Corresponding author

Contents

1	Introduction	2
2	S_3 Quantum Double Phase in the S_3 Enlarged HGW String-Net Model	3
3	Enriching the S_3 Quantum Double with EM-Exchange Symmetry	5
4	Symmetry Transformation and Fragmentation of the S_3 Quantum Double Anyons	6
4.1	Symmetry Transformation Through Domain Wall	6
4.2	Nonlinear Representation of the EM-Exchange Symmetry	9
5	Discussion	12
A	String-net Model	13
A.1	Topological Features	15
A.2	Excited States	16
A.3	The Output UMTC is the Center of the Input UFC	18
A.4	The String-Net Model with Non-Commutative Input UFCs	19
B	The Anyon Species of S_3 Quantum Double Phase	21
C	Multi-fusion Category as the Input of SET Model	21
C.1	Input data: A Multifusion Category with Associated Isomorphisms	22
C.2	Hamiltonian	23
D	The Categorical Data of \mathbb{Z}_2 Symmetry Enriched S_3 Multi-fusion Category	24
D.1	The Fusion Rules	24
D.2	The $6j$ -Symbols	24
E	The anyon Spectrum of EM-Exchange Symmetry Enriched S_3 String-net Model	25
F	Anyon Fragmentation Pattern	29
G	Proof that ρ^G and ρ^H are not projective representations	29

1 Introduction

Symmetry-enriched topological (SET) phases arise when topological phases are endowed with global symmetries[10–23], yielding structures believed to extend beyond both the Landau–Ginzburg paradigm¹[24–26] and ordinary topological order. When topological phases and symmetries interplay in SET phases, more structures emerge[12, 16–18, 27], greatly enriching the landscape of possible quantum phases and having important implications for both theoretical classification schemes[17, 18, 28, 29] and practical applications.

SET phases may be classified by symmetry fractionalizations[18, 21, 30–35]; however, symmetry fractionalizations in general do not directly correspond to how anyons are transformed under global symmetries[18], especially for non-Abelian anyons. Symmetry transformations of non-Abelian anyons in SET phases remain elusive. The key point lies in the internal gauge spaces of non-Abelian anyons: Unlike Abelian anyons, which are 1-dimensional, non-Abelian anyons may carry multiple flux types and gauge charge sectors[2, 7, 36, 37]—and thus bearing multi-dimensional nontrivial internal Hilbert spaces and transforming under symmetry in sophisticated ways—not merely acquiring a phase factor—under a global symmetry action.

Therefore, it is essential to explicitly account for the internal spaces of non-Abelian anyons in order to describe their transformations under global symmetry actions. Nevertheless, conventional TQFT approaches treat anyons as abstract simple objects in a modular tensor category[1, 38], hiding their internal gauge structures. Our recent construction of the enlarged Hu-Geer-Wu (HGW) string-net model of topological phases[8] made it possible to explicitly formulate and investigate non-Abelian anyons’ internal spaces and is further extended to a model of SET phases[8, 9]. By means of these internal gauge spaces of anyons, we show rich structures of symmetry actions emerge on non-Abelian topological orders.

In our work, we employ this string-net model of SET phases (see Sections II and III) to probe the global-symmetry actions on non-Abelian anyons. Although our approach is generic, to be concrete, we consider a specific example of the S_3 quantum-double phase enriched by its electromagnetic-exchange (\mathbb{Z}_2) symmetry. We find that under EM-exchange symmetry, the two non-Abelian types, C and F , are permuted, while the other non-Abelian anyon types remain invariant under the symmetry. Nevertheless, these non-Abelian anyons’ multi-dimensional internal Hilbert spaces undergo nontrivial global symmetry transformations: The internal Hilbert spaces of certain types of anyons may fragment into eigensubspaces labeled by distinct (and generally fractional) global symmetry charges. Crucially, these transformations cannot be captured by ordinary linear or projective representations—instead, they realize genuinely nonlinear representations arising from the categorical symmetry nature of the EM-exchange symmetry of the S_3 quantum-double topological phase. As for the pair of anyon types permuted under the EM-exchange symmetry, their internal spaces are hybridized and then fragmented according to global symmetry rather than anyon types. We call this ubiquitous mechanism global symmetry fragmentation (GSF).

¹A recent paper by two of us[8] shows that topological phases and their phase transitions can be encompassed by a generalized Landau-Ginzburg Paradigm.

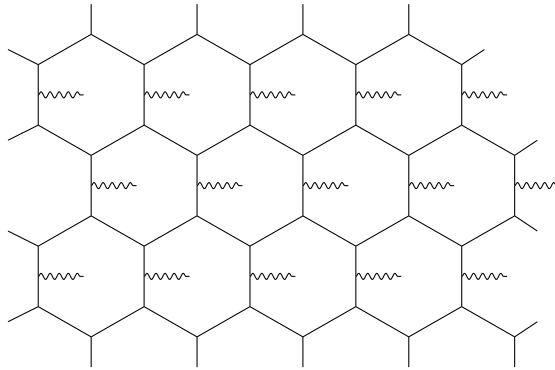


Figure 1: Part of the string-net model lattice. A tail (wavy line) is attached to an arbitrary edge of each plaquette.

Our findings establish nonlinear symmetry fragmentation as a universal feature of non-Abelian SET phases. Understanding how global symmetries enrich non-Abelian topological phases not only deepens our theoretical understanding of SET phases but also may offer new insights and means of realizing universal topological quantum computation—particularly given recent evidence that S_3 quantum double model can support universal quantum computation[39]—and suggests routes for engineering novel symmetry-enriched quantum materials.

2 S_3 Quantum Double Phase in the S_3 Enlarged HGW String-Net Model

In this section we briefly introduce the $D(S_3)$ topological phase realized in the enlarged HGW string-net model[8] with input UFC $\text{Vec}(S_3)$. This model is a lattice gauge theory coupled with anyonic matter defined on a 2-dimensional trivalent spatial lattice. Each plaquette has a tail anchored to one of its edges². Each edge/tail is oriented and labeled by a group element in

$$S_3 = \{1, r, r^2, s, sr, rs : r^3 = s^2 = (sr)^2 = 1\},$$

which is the configuration space of the gauge field. Reversing the orientation of an edge/tail while inverting the group element on it does not change the gauge field configuration. The gauge-field Hilbert space is spanned by all possible gauge-field configurations, obeying the group multiplication rules of S_3 at any vertex: Let i, j , and k are respectively the group elements on the three edges incident counterclockwise at a vertex (assuming each edge is oriented towards the vertex; if not, reversing both its orientation and group element), the multiplication $ijk = 1 \in S_3$ must hold.

In the enlarged HGW string-net model, the S_3 lattice gauge field couples to the eight types of $D(S_3)$ anyons, denoted as A, B, C, D, E, F, G, H , which are the matter fields residing in plaquettes. Because S_3 is non-Abelian, several types of anyons are *non-Abelian*,

²The original string-net model in Ref. [24], which has no such tails, cannot fully describe charge excitations. These added tails carry anyons' charges, thus enlarging the Hilbert space to encompass the complete anyon spectrum of the model.

each occupying a multi-dimensional internal gauge space, analogous to the colour spaces of quarks[40–45]. Nevertheless, standard TQFTs overlook the internal gauge dofs because they treat each anyon as a structureless simple object in a modular tensor category. For a generic J -type anyon in a plaquette, its internal basis states are labeled by a pair (p, α) . Here, $p \in S_3$ is the **flux type** that sources the gauge curvature in the plaquette via the magnetic Gauss law, which dictates a commensurate gauge-field configuration on the tail in the plaquette. A flux type p may have an associated charge space, spanned by the label $1 \leq \alpha \leq \dim(\text{Charge space})$. In the current example, a charge space is in fact representation space of S_3 . Abelian anyons only have a unique flux type p and one-dimensional charge space, while a non-Abelian anyon may admit several fluxes and/or a multi-dimensional charge space. Such internal spaces transform covariantly under local gauge transformations [8].

Table 1 records the 8 $D(S_3)$ anyon types, their fluxes, and internal-space basis.

Anyon Species	A	B	C	D	E	F	G	H
Fluxes (Valued in S_3)	1	1	1	s, rs, sr	s, rs, sr	r, r^2	r, r^2	r, r^2
Charge Space Dimension	1	1	2	1	1	1	1	1
Gauge Space Dimension	1	1	2	3	3	2	2	2
Internal-Space Basis	1	1	$1_1, 1_2$	s, rs, sr	s, rs, sr	r, r^2	r, r^2	r, r^2

Table 1: Anyon species of $D(S_3)$ phase

In a pure topological phase, an anyon’s internal states are not observable, as they would transform as the anyon hops on the lattice and inevitably interacts with the gauge field. The only gauge-invariant quantity or the physical observable of an anyon is the anyon type.

The $D(S_3)$ anyon braiding and self statistics are captured by the corresponding modular S and T matrices:

$$S = \frac{1}{6} \begin{pmatrix} 1 & 1 & 2 & 3 & 3 & 2 & 2 & 2 \\ 1 & 1 & 2 & -3 & -3 & 2 & 2 & 2 \\ 2 & 2 & 4 & 0 & 0 & -2 & -2 & -2 \\ 3 & -3 & 0 & 3 & -3 & 0 & 0 & 0 \\ 3 & -3 & 0 & -3 & 3 & 0 & 0 & 0 \\ 2 & 2 & -2 & 0 & 0 & 4 & -2 & -2 \\ 2 & 2 & -2 & 0 & 0 & -2 & -2 & 4 \\ 2 & 2 & -2 & 0 & 0 & -2 & 4 & -2 \end{pmatrix}, \quad T = \begin{pmatrix} 1 & 0 & 0 & 0 & 0 & 0 & 0 & 0 \\ 0 & 1 & 0 & 0 & 0 & 0 & 0 & 0 \\ 0 & 0 & 1 & 0 & 0 & 0 & 0 & 0 \\ 0 & 0 & 0 & 1 & 0 & 0 & 0 & 0 \\ 0 & 0 & 0 & 0 & -1 & 0 & 0 & 0 \\ 0 & 0 & 0 & 0 & 0 & 1 & 0 & 0 \\ 0 & 0 & 0 & 0 & 0 & 0 & e^{\frac{2\pi i}{3}} & 0 \\ 0 & 0 & 0 & 0 & 0 & 0 & 0 & e^{-\frac{2\pi i}{3}} \end{pmatrix}. \quad (2.1)$$

Note that any global symmetry permissible on a topological phase must preserve the S and T matrices of the phase. Seen from the modular S and T matrices above, we can see that there the $D(S_3)$ phase admits a Z_2 symmetry that exchanges its anyon types C and F , while preserving all other anyon types. Since the C -type anyon has only a trivial flux but a 2-dimensional charge space, while the F -type anyon has two flux type but trivial charge space, this Z_2 symmetry is an EM-exchange symmetry.

3 Enriching the S_3 Quantum Double with EM-Exchange Symmetry

In this section, we describe how to extend the enlarged HGW model describing the $D(S_3)$ phase to a model describing the EM-exchange symmetry enriched $D(S_3)$ phase. We focus on this particular example, while the general construction is reported in a companion paper[9].

It is known that the original Levin-Wen string-net model can describe SET phases upon replacing its input UFCs by multifusion categories[16–18]. Nevertheless, such constructions have two limitations. First, they cannot manifest anyons' internal spaces, thereby unable to investigate symmetry actions on non-Abelian anyons properly. Second, they require a manual input of the global symmetries to be endowed on the topological phases rather than using only the input UFCs of the string-net model. Our SET model overcomes these two shortcomings because (1) it is based on the enlarged HGW model that manifests anyons' internal spaces by construction, and (2) it extracts the input multifusion categories from the original input UFCs of the enlarged HGW model without *ad hoc* knowledge of the global symmetries to be endowed.

In our companion work[9], we can first construct multifusion categories, each equipped with an appropriate isomorphism (necessary for defining symmetry sectors), from the input UFC \mathcal{F} of the enlarged HGW model. Then, by replacing \mathcal{F} with one of these derived multifusion category together with a chosen isomorphism as the input data of the enlarged HGW model, we obtain a lattice exactly solvable model of an SET phase. This model is reviewed in Appendix C.

Such a multifusion category is constructed from the irreducible bimodules over the Frobenius algebra objects of \mathcal{F} . The technical details can be found in Ref. [9]. Here, we focus on the case where $\mathcal{F} = \mathbf{Vec}(S_3)$, as described in the previous section. For the model describing the EM-exchange symmetry enriched $D(S_3)$ phase, we directly adopt from Ref. [9] the corresponding input multifusion category equipped with the necessary isomorphism derived from $\mathbf{Vec}(S_3)$. This multifusion category can be arranged in a 2×2 matrix:

$$\mathcal{M} = \begin{pmatrix} \{1_{++}, r_{++}, r_{++}^2, s_{++}, r s_{++}, s r_{++}\} & \{\alpha_{+-}, \beta_{+-}\} \\ \{\alpha_{-+}, \beta_{-+}\} & \{1_{--}, r_{--}, r_{--}^2, s_{--}, r s_{--}, s r_{--}\} \end{pmatrix}. \quad (3.1)$$

The fusion rules and $6j$ -symbols of this multifusion category can be found in Appendix D. As explained in Appendix C, the two diagonal sets of elements of the multi-fusion matrix \mathcal{M} , i.e., $\{1_{++}, r_{++}, r_{++}^2, s_{++}, r s_{++}, s r_{++}\}$ and $\{1_{--}, r_{--}, r_{--}^2, s_{--}, r s_{--}, s r_{--}\}$, are two UFCs isomorphic to each other and are both isomorphic to $\mathbf{Vec}(S_3)$. They are respectively

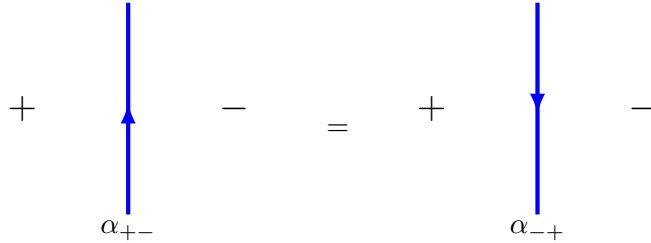


Figure 2: Domain wall

the sets of the basic degrees of freedom of the two different symmetry sectors, labeled by $+$ and $-$, related by the EM-exchange symmetry. The off-diagonal sets in \mathcal{M} are the domain-wall degrees of freedom defined as follows. A domain wall between symmetry sectors $+$ and $-$ is oriented (see Fig. 2): With respect to the orientation, on the domain wall's left and right are always respectively the $+$ and $-$ sectors, so the corresponding domain-wall degree of freedom take value in the set $\{\alpha_{+-}, \beta_{+-}\}$. If we reverse the orientation of the domain wall, its degree of freedom should instead take value in $\{\alpha_{-+}, \beta_{-+}\}$. The EM-exchange symmetry transformation operator swaps the 2 sectors:

$$\mathcal{G} : a_{ij} \rightarrow a_{i\bar{j}}, \quad \forall a \in \{1, r, r^2, s, rs, sr\}, \quad i, j \in \{+, -\}, \quad (3.2)$$

where, $\bar{+} = -$, $\bar{-} = +$.

The SET model still has anyon excitations, which can be extracted from the half braiding z -tensor of the multifusion category (3.1), as shown in Appendix E. More importantly, we can read off directly from the z -tensors how the $D(S_3)$ anyons are transformed under the symmetry. For example, when an anyon C in the $+$ sector hops into the $-$ sector, it becomes anyon F . Let's look into the details.

4 Symmetry Transformation and Fragmentation of the S_3 Quantum Double Anyons

Now are ready to study how the EM-exchange symmetry acts on the $D(S_3)$ phase and transform the anyons therein in detail. The phenomenon global symmetry fragmentation will surface naturally.

4.1 Symmetry Transformation Through Domain Wall

As different symmetry sectors differ by a symmetry transformation, we can say that when an anyon in one symmetry sector crosses a domain wall and enters another symmetry sector, it undergoes a symmetry transformation, conducted by the domain wall, as depicted in Figure 3. For example, a C (an F) anyon in sector $+$ upon crossing a domain wall would be transformed into an F (a C) anyon in sector $-$. The conventional methods of studying SET phases would have to stop at this level of understanding the symmetry transformations of non-Abelian anyons. Nonetheless, by means of our domain wall constructed in the enlarged HGW model, explicit transformations on anyons' internal spaces can be revealed.

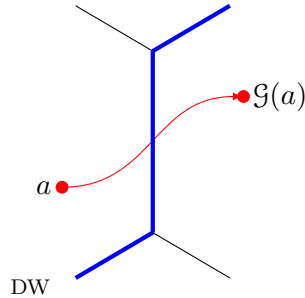


Figure 3: Anyon a crossing a domain wall (blue thick line) undergoes a symmetry transformation and becomes anyon $\mathcal{G}(a)$. Red horizontal line represents the anyon's hopping path.

As aforementioned, an anyon's internal states are changing when the anyon hops on the lattice. So, to focus only on global symmetry transformations on an anyon's internal space, we should consider the scenario where the anyon resides right in a plaquette right beside a domain wall, then crosses the domain wall into the plaquette on the other side, and stops there.

Back to the EM-exchange symmetry enriched $D(S_3)$ phase. Although according to Eq. (3.1), apparently there are two types of domain walls labeled by α and β , they in fact differ by a \mathbb{Z}_2 gauge generated by the gauge degree of freedom $s \in S_3$ with $s^2 = 1$. [9]. As such, if we know the symmetry transformations on the anyons conducted by crossing domain wall α , we can easily derive those conducted by crossing domain wall β . Hence, hereafter, we would consider domain wall α only unless otherwise mentioned. The EM-exchange symmetry transformations on the $D(S_3)$ anyons can be directly read off from the z -tensors (Appendix E) of the SET model. For instance, from $z_{r_{++},(1_1)_{--},\alpha_{+-}}^{(F,C);\alpha_{+-}} = 1$, we can see that under symmetry transformation, F_r transforms into C_{1_1} . We record all these transformations in Table 2, which gives the representations $\rho^J(\mathcal{G}_{em})$ of the symmetry transformation \mathcal{G}_{em} over anyon J (while for any anyon J the representation of trivial action 1 is trivial: $\rho^J(1) = \mathbb{1}$). Note that here, J may not be a single anyon type of $D(S_3)$ because as seen, the EM-exchange symmetry can mix anyon types C and F . As such, in the following, we would also consider $J = C \oplus F$, which is a nonsimple object in $D(S_3)$. For example

$$\rho^D(\mathcal{G}_{em}) = \frac{1}{\sqrt{3}} \begin{pmatrix} 1 & 1 & 1 \\ 1 & e^{i\frac{2\pi}{3}} & e^{-i\frac{2\pi}{3}} \\ 1 & e^{-i\frac{2\pi}{3}} & e^{i\frac{2\pi}{3}} \end{pmatrix}. \quad (4.1)$$

This result leads to three observations:

1. Abelian anyons A and B are the symmetry singlets. So, they remain well-defined anyons in the SET phase, as indicated in the SET's z -tensors (Appendix E).
2. Certain non-Abelian anyons' internal spaces are fragmented into subspaces as eigenspaces of the symmetry action. For example, the internal space of anyon H is fragmented into

$D(S_3)$ Anyon Internal Basis States	EM-exchange symmetry transformation
A	A
B	B
C_{1_1}	F_r
C_{1_2}	F_{r^2}
F_r	C_{1_1}
F_{r^2}	C_{1_2}
G_r	$e^{i\frac{2\pi}{3}} G_r$
G_{r^2}	$e^{i\frac{2\pi}{3}} G_{r^2}$
H_r	$e^{-i\frac{2\pi}{3}} H_{r^2}$
H_{r^2}	$e^{-i\frac{2\pi}{3}} H_r$
D_s	$\frac{1}{\sqrt{3}}(D_s + D_{rs} + D_{sr})$
D_{rs}	$\frac{1}{\sqrt{3}}(D_s + e^{i\frac{2\pi}{3}} D_{rs} + e^{-i\frac{2\pi}{3}} D_{sr})$
D_{sr}	$\frac{1}{\sqrt{3}}(D_s + e^{-i\frac{2\pi}{3}} D_{rs} + e^{i\frac{2\pi}{3}} D_{sr})$
E_s	$\frac{1}{\sqrt{3}}(E_s + E_{rs} + E_{sr})$
E_{rs}	$\frac{1}{\sqrt{3}}(E_s + e^{i\frac{2\pi}{3}} E_{rs} + e^{-i\frac{2\pi}{3}} E_{sr})$
E_{sr}	$\frac{1}{\sqrt{3}}(E_s + e^{-i\frac{2\pi}{3}} E_{rs} + e^{i\frac{2\pi}{3}} E_{sr})$

Table 2: EM-exchange symmetry transformations on the internal states of $D(S_3)$ anyons, as conducted by hopping the anyons across an α -type domain wall. Here, J_x , where J is an anyon type, and x is a internal basis label, is a shorthand notation of an internal state of a J -type anyon.

two symmetry eigenstates: $H_r + H_{r^2}$ and $H_r - H_{r^2}$, with definite symmetry charges $\frac{2}{3}$ and $\frac{1}{6}$. (We will explain the nature of these charges in the next subsection.) We dub this phenomenon on non-Abelian anyons *global symmetry fragmentation*, which is common in any symmetry-enriched non-Abelian topological phases. An exception is the G type, whose internal space is not fragmented; rather, a G -type anyon as a whole acquires a global symmetry charge of $1/3$. The fragmentation of type- D and E anyons are somewhat more involved but can be easily derived from the z -tensors in Appendix E and is shown in Appendix F. It's worth of note that the symmetry fragmentation pattern in an SET phase is gauge dependent. As we mentioned ear-

lier, the EM-exchange symmetry transformations can be defined as conducted by the β -type domain wall (called the β -gauge), which is related to those in Table 2 by the α -type domain wall (the α -gauge). If we take the β -gauge, it would be the G -type anyons acquire fragmentation, while the H -type not fragmented.

3. Anyons C and F are exchanged. More concretely, their internal spaces are mixed up: $C_{1_1} \pm F_r$ and $C_{1_2} \pm F_{r^2}$. So, the mixed internal spaces of C and F are fragmented into two 2-dimensional eigenspaces of the symmetry:

$$\text{span}\{C_{1_1} + F_r, C_{1_2} + F_{r^2}\},$$

with charge 0, and

$$\text{span}\{C_{1_1} - F_r, C_{1_2} - F_{r^2}\},$$

with charge 1/2.

4.2 Nonlinear Representation of the EM-Exchange Symmetry

We have attributed to the fragmented internal spaces of anyons fractional symmetry charges; however, what is the nature of these charges? Do these charges label certain linear or projective representations of the symmetry group? We now address these questions. In the current example, clearly these charges do not correspond to any linear or projective representations of the EM-exchange symmetry because the symmetry group is \mathbb{Z}_2 , which has linear representations labeled by integers only and has no projective representations at all. In fact, the fractional charges we have found label nonlinear representations of \mathbb{Z}_2 . This can be shown by composing two consecutive symmetry transformations on the $D(S_3)$ anyons as follows.

Since the symmetry transformations are conducted by hopping the anyons cross a domain wall, composing two such transformations on an anyon should be hopping the anyon cross 2 domain walls, as seen in Figure 4. In Figure 4(a), as pointed out in the figure caption, Pachner moves³ are invoked in composing the two hoppings; accordingly, composing the corresponding two symmetry formations must involve the effects of the Pachner moves and thus cannot be directly multiplying the two representation matrices⁴ of the two transformations.

In our EM-exchange symmetry enriched S_3 quantum double phase, composing two nontrivial symmetry transformations reads

$$\mathcal{G}_{em}^J \circ \mathcal{G}_{em}^J := \sum_b \omega_{ab} \rho_{ab}^J(\mathcal{G}_{em}) \rho_{bc}^J(\mathcal{G}_{em}), \quad (4.2)$$

which gives that

$$\sum_b \omega_{ab} \rho_{ab}^J(\mathcal{G}_{em}) \rho_{bc}^J(\mathcal{G}_{em}) = \rho_{ac}^J(1) = \mathbb{1}, \quad (4.3)$$

³Pachner moves are topological moves. See Appendix A.1.

⁴Note that nonlinear representations are not matrices; however, here we assume a section in the representation bundle is chosen for us to express the representation as matrices. The nonlinearity is manifest in the composition of two symmetry transformations.

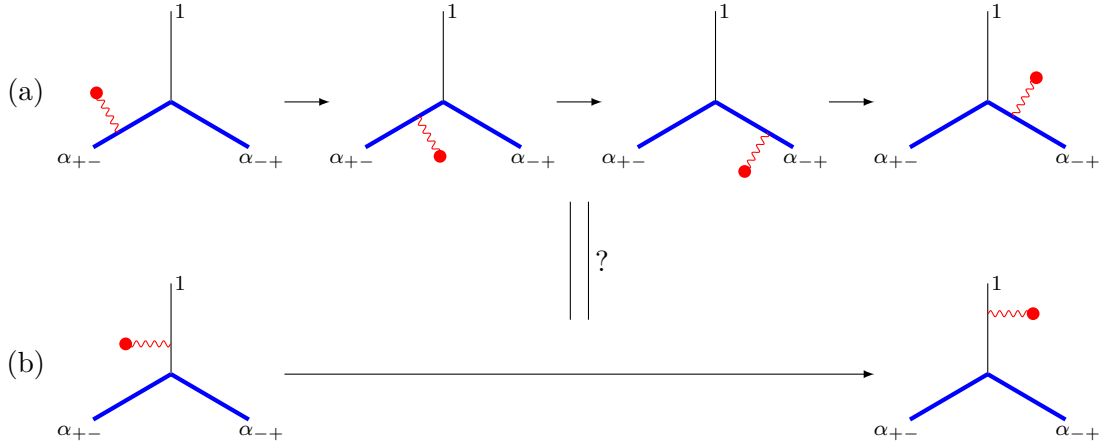


Figure 4: The composition of symmetry transformations, which is equivalent as the anyon crosses two domain wall (blue thick line). The orientation of the edges are all set to be going upward.

where matrices $\rho^J(\mathcal{G}_{em})$, e.g., (4.1), can be extracted from Table 2. Here, ω is a rank-2 tensor, which is due to the Pachner moves and is independent of anyon type J . Non-zero elements of ω are

$$\begin{aligned}
\omega_{1,r} &= \omega_{1,r^2} = \omega_{1,s} = \omega_{1,rs} = \omega_{1,sr} = 1, \\
\omega_{s,r} &= \omega_{s,r^2} = \omega_{s,rs} = \omega_{s,sr} = 1, \\
\omega_{r,r} &= \omega_{r^2,r^2} = \omega_{rs,rs} = \omega_{sr,sr} = e^{i\frac{2\pi}{3}}, \\
\omega_{r,r^2} &= \omega_{rs,sr} = e^{-i\frac{2\pi}{3}}.
\end{aligned} \tag{4.4}$$

As opposed to the case of projective representations, ω is not a phase factor associated with an entire matrix $\rho^J(\mathcal{G}_{em})$ but has different components for different matrix elements of $\rho^J(\mathcal{G}_{em})$. Therefore, the representations ρ^J are neither linear nor projective, but nonlinear representations of the EM-exchange symmetry. The fractional charges carried by the fragmented internal spaces of $D(S_3)$ anyons precisely label the irreducible nonlinear representations. A basis transformation must be applied to an anyon's internal space to manifest the fragmentation and the corresponding irreducible nonlinear representations. To be specific, we consider the following instances.

Here we provide 3 examples:

1. According to Table 2, for $J = H$, the basis states H_r and H_{r^2} are exchanged under the symmetry transformation. Hence, the representation ρ^H can be decomposed into two 1-dimensional representations ρ^{H+} and ρ^{H-} , where $H_+ = h_r + H_{r^2}$, $H_- = H_r - H_{r^2}$. We have $\rho^{H+}(\mathcal{G}_{em}) = e^{-i\frac{2\pi}{3}}$, $\rho^{H-}(\mathcal{G}_{em}) = e^{i\frac{\pi}{3}}$, such that (4.3) in this case reads

$$\begin{aligned}
\rho^{H+}(\mathcal{G}_{em})\rho^{H+}(\mathcal{G}_{em}) &= e^{i\frac{2\pi}{3}}\rho^{H+}(1); \\
\rho^{H-}(\mathcal{G}_{em})\rho^{H-}(\mathcal{G}_{em}) &= e^{i\frac{2\pi}{3}}\rho^{H-}(1).
\end{aligned} \tag{4.5}$$

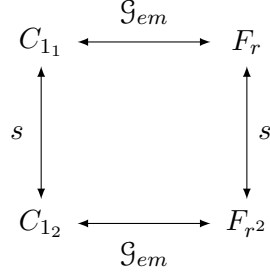


Figure 5: Symmetry transformation \mathcal{G}_{em} and gauge transformation s in the fragmented $C \oplus F$ space.

One might then mistake the irreducible representations ρ^{H+} and ρ^{H-} as projective representations of \mathbb{Z}_2 and further regard them as linear representations because any apparent projective representation of \mathbb{Z}_2 is equivalent to a linear representation because $H^2(\mathbb{Z}_2, U(1)) = \{0\}$. Nevertheless, as in Appendix G, we can show that ρ^{H+} and ρ^{H-} can never be made equivalent to linear representations of \mathbb{Z}_2 . Thus, H is indeed fragmented into two nontrivial nonlinear representations of \mathbb{Z}_2 characterized by charges $2/3$ and $1/6$. Now we have seen the true meaning of these charges, which were first inferred in Table 2.

2. If $J = G$, the two basis states G_r and G_r^2 both acquire a phase factor $e^{i\frac{2\pi}{3}}$ under the symmetry action. So, (4.3) now reads

$$\begin{aligned}
\rho^{G_r}(\mathcal{G}_{em})\rho^{G_r}(\mathcal{G}_{em}) &= e^{-i\frac{2\pi}{3}}\rho^{G_r}(1); \\
\rho^{G_{r,2}}(\mathcal{G}_{em})\rho^{G_{r,2}}(\mathcal{G}_{em}) &= e^{-i\frac{2\pi}{3}}\rho^{G_{r,2}}(1).
\end{aligned} \tag{4.6}$$

Likewise in Appendix G, we can show that the composition of symmetry transformations above indeed signifies a nonlinear representation of \mathbb{Z}_2 . One might however misconceive that G 's internal space is also fragmented to two copies of the same 1-dimensional nonlinear representation. In fact, as the basis states G_r and $G_{r,2}$ are always interchangeable under G 's internal gauge, they are not physically distinguishable. Therefore, one should regard the 2-dimensional internal space of G as an indecomposable 2-dimensional nonlinear representation space of \mathbb{Z}_2 characterized by the phase factor $e^{i\frac{2\pi}{3}}$ or charge $1/3$.

3. More interestingly is the case where $J = C \oplus F$. The 4-dimensional representation $\rho^{C \oplus F}$ could be decomposed into two 2-dimensional representations $\rho^{(C \oplus F)+}$ and $\rho^{(C \oplus F)-}$, where

$$\begin{aligned}
V_{(C \oplus F)+} &= \text{span}\{C_{1_1} + F_r, C_{1_2} + F_{r,2}\}, \\
V_{(C \oplus F)-} &= \text{span}\{C_{1_1} - F_r, C_{1_2} - F_{r,2}\},
\end{aligned} \tag{4.7}$$

such that $\rho^{(C \oplus F)+}(\mathcal{G}_{em}) = \mathbb{1}$ and $\rho^{(C \oplus F)-}(\mathcal{G}_{em}) = -\mathbb{1}$. These two 2-dimensional representations are irreducible for the following reason. Since the internal gauges of

$C(F)$ can mix $C_{1_1}(F_r)$ and $C_{1_2}(F_{r_2})$, we cannot differentiate $C_{1_1} + F_r(C_{1_1} - F_r)$ from $C_{1_2} + F_{r_2}(C_{1_2} - F_{r_2})$. As such, all states in the 2-dimensional space $V_{(C \oplus F)_+}$ ($V_{(C \oplus F)_-}$) carry the same symmetry charge 0 (1/2), rendering the space a degenerate eigenspace of the symmetry action. The composition rule (4.3) now takes the form

$$\begin{aligned} \rho^{(C \oplus F)_+}(\mathcal{G}_{em})\rho^{(C \oplus F)_+}(\mathcal{G}_{em}) &= \rho^{(C \oplus F)_+}(1); \\ \rho^{(C \oplus F)_+}(\mathcal{G}_{em})\rho^{(C \oplus F)_+}(\mathcal{G}_{em}) &= \rho^{(C \oplus F)_+}(1). \end{aligned} \tag{4.8}$$

Therefore, it is clear that when the $D(S_3)$ phase is endowed with the EM-exchange symmetry, certain types of its non-Abelian anyons do transform and fragment into nonlinear representations under the symmetry. This justifies the terminology *nonlinear symmetry Fragmentation* of nonabelian anyons. The EM-exchange symmetry is essentially \mathbb{Z}_2 , which appears to be an innocent group symmetry; however, it is in fact a categorical symmetry, which is reflected in its nonlinear representations that amalgamate the \mathbb{Z}_2 group nature and the $\text{Vec}(S_3)$ categorical nature via the $6j$ symbols. By the systematic construction of lattice models of SET phases done in our companion paper[9], nonlinear symmetry fragmentation is a general feature of symmetry-enriched non-Abelian topological phases.

5 Discussion

In this paper, for the first time in the literature to date, we have explicitly studied the global symmetry action on non-Abelian anyons in an SET phase—the S_3 quantum double phase enriched by the EM-exchange symmetry. We discovered the phenomenon of nonlinear symmetry fragmentation by exemplifying how $D(S_3)$ non-Abelian anyons’s internal spaces are rearranged and decomposed into nonlinear irreducible representations of the EM-exchange (a \mathbb{Z}_2) symmetry. This phenomenon is not unique to the S_3 quantum double phase enriched by the EM-exchange symmetry but ubiquitous in SET phases involving non-Abelian topological phases. A recent work[39] shows that the $D(S_3)$ non-Abelian anyons can support universal quantum computation. Since now we have a finer understanding of how such anyons behave in a richer phase—the $D(S_3)$ enriched by the EM-exchange symmetry, it would be interesting to explore the utility of nonlinear symmetry fragmentation for topological quantum computation, such as improving gate and/or algorithm efficiency by harnessing the power of global symmetries.

Furthermore, we have not seen a non-Abelian topological phase enriched by a non-Abelian global symmetry. A possible example is the D_4 quantum double phase enriched by the permutation symmetry S_3 . It would be illuminating to study the interplay between the non-Abelian anyons and the non-Abelian global symmetry in such examples. Even more exotically, if a non-Abelian topological phase is endowed with not a group but an algebraic global symmetry, how would the non-Abelian anyons therein transform under the global symmetry? How would the concept of nonlinear symmetry fragmentation be generalised in such cases?

Acknowledgments

The authors thank Hongguang Liu, Yuting Hu, and Yifei Wang for inspiring and helpful discussions. YW is supported by NSFC Grant No. KRH1512711, the Shanghai Municipal Science and Technology Major Project (Grant No. 2019SHZDZX01), Science and Technology Commission of Shanghai Municipality (Grant No. 24LZ1400100), and the Innovation Program for Quantum Science and Technology (No. 2024ZD0300101). The authors are grateful for the hospitality of the Perimeter Institute during his visit, where the main part of this work is done. This research was supported in part by the Perimeter Institute for Theoretical Physics. Research at Perimeter Institute is supported by the Government of Canada through the Department of Innovation, Science and Economic Development and by the Province of Ontario through the Ministry of Research, Innovation and Science.

A String-net Model

In this section, we briefly review the string-net model defined in Ref. [5], which was adapted from that in [2]. The string-net model is an exactly solvable model defined on a 2-dimensional lattice. An example lattice is depicted in Fig. 1. All vertices are trivalent. Within each plaquette of the lattice, a tail is attached to an arbitrary edge of the plaquette, pointing inward. We will demonstrate that different choices of the edge to which the tail is attached are equivalent in Appendix A.1. Each edge and tail is oriented, but we'll show that different choices of directions are equivalent.

The input data of the string-net model is a unitary fusion category \mathcal{F} , described by a finite set $L_{\mathcal{F}}$, whose elements are called *simple objects*, equipped with three functions $N : L_{\mathcal{F}}^3 \rightarrow \mathbb{N}$, $d : L_{\mathcal{F}} \rightarrow \mathbb{R}^+$, and $G : L_{\mathcal{F}}^6 \rightarrow \mathbb{C}$. The function N sets the *fusion rules* of the simple objects, satisfying

$$\sum_{e \in L_{\mathcal{F}}} N_{ab}^e N_{ec}^d = \sum_{f \in L_{\mathcal{F}}} N_{af}^d N_{bc}^f, \quad N_{ab}^c = N_{c^*a}^{b^*}.$$

There exists a special simple object $1 \in L_{\mathcal{F}}$, called the *trivial object*, such that for any $a, b \in L_{\mathcal{F}}$,

$$N_{1a}^b = N_{1b}^a = \delta_{ab},$$

where δ is the Kronecker symbol. For each $a \in L_{\mathcal{F}}$, there exists a unique simple object $a^* \in L_{\mathcal{F}}$, called the *opposite object* of a , such that

$$N_{ab}^1 = N_{ba}^1 = \delta_{ba^*}.$$

We only consider the case where for any $a, b, c \in L_{\mathcal{F}}$, $N_{ab}^c = 0$ or 1. In this case, we define

$$\delta_{abc} = N_{ab}^{c^*} \in \{0, 1\}.$$

The basic configuration of the string-net model is established by labeling each edge and tail with a simple object in $L_{\mathcal{F}}$, subject to the constraint on all vertices that $\delta_{ijk} = 1$ for

the three incident edges or tails meeting at this vertex, all pointing toward the vertex and respectively counterclockwise labeled by $i, j, k \in L_{\mathcal{F}}$. We can reverse the direction of any edge or tail and simultaneously conjugate its label as $j \rightarrow j^*$, which keeps the configuration invariant. The Hilbert space \mathcal{H} of the model is spanned by all possible configurations of these labels on the edges and tails.

The function $d : L_{\mathcal{F}} \rightarrow \mathbb{R}^+$ returns the *quantum dimensions* of the simple objects in $L_{\mathcal{F}}$. It is the largest eigenvalues of the fusion matrix and forms the 1-dimensional representation of the fusion rule.

$$d_a d_b = \sum_{c \in L_{\mathcal{F}}} N_{ab}^c d_c.$$

In particular, $d_1 = 1$, and for any $a \in L_{\mathcal{F}}$, $d_a = d_{a^*} \geq 1$.

The function $G : L_{\mathcal{F}}^6 \rightarrow \mathbb{C}$ defines the *6j-symbols* of the fusion algebra. It satisfies

$$\begin{aligned} \sum_n d_n G_{u^*u^*a}^{pqn} G_{j^*i^*b}^{u^*v^n} G_{q^*p^*c}^{ijn} &= G_{i^*pu^*}^{abc} G_{vq^*j^*}^{c^*b^*a^*}, & \sum_n d_n G_{kln}^{ijp} G_{l^*k^*n}^{j^*i^*q} &= \frac{\delta_{pq^*}}{d_p} \delta_{ijp} \delta_{klq}, \\ G_{kln}^{ijm} = G_{ijn^*}^{klm^*} = G_{lkn^*}^{jim} = G_{nk^*l^*}^{mij} &= \alpha_m \alpha_n \overline{G_{l^*k^*n^*}^{j^*i^*m^*}}, & |G_{1bc}^{abc}| &= \frac{1}{\sqrt{d_b d_c}} \delta_{abc}, \end{aligned} \quad (\text{A.1})$$

where $\alpha_m = G_{1m^*m}^{1mm^*} \in \{\pm 1\}$ is the Frobenius-Schur indicator of simple object m .

The Hamiltonian of the string-net model reads

$$H := - \sum_{\text{Plaquettes } P} Q_P, \quad Q_P := \frac{1}{D} \sum_{s \in L_{\mathcal{F}}} d_s Q_P^s, \quad (\text{A.2})$$

where operator Q_P^s acts on edges surrounding plaquette P and has the following matrix elements on a hexagonal plaquette:

$$Q_P^s := \delta_{p,1} \delta_{j_1, j_7} \sum_{j_k \in L_{\mathcal{F}}} \prod_{k=1}^6 \left(\sqrt{d_{i_k} d_{j_k}} G_{s j_{k+1}^*}^{e_k i_k i_{k+1}^*} \right),$$

and

$$D := \sum_{a \in L_{\mathcal{F}}} d_a^2$$

is the total quantum dimension of UFC \mathcal{F} . Here, we only show the actions of the Q_P operator on a hexagonal plaquette. The matrix elements of Q_P operators on other types of plaquettes are defined similarly. We also omit the “ $|\cdot\rangle$ ” labels surrounding all diagram for simplicity, unless they are specifically required.

It turns out that

$$(Q_P^s)^\dagger = Q_P^{s^*}, \quad Q_P^r Q_P^s = \sum_{t \in L_{\mathcal{F}}} N_{rs}^t Q_P^t, \quad Q_P^2 = Q_P, \quad Q_{P_1} Q_{P_2} = Q_{P_2} Q_{P_1}.$$

The summands Q_P in Hamiltonian H are commuting projectors, so the Hamiltonian is exactly solvable. The ground-state subspace \mathcal{H}_0 of the system is the projection

$$\mathcal{H}_0 = \left[\prod_{\text{Plaquettes } P} Q_P \right] \mathcal{H}. \quad (\text{A.3})$$

If the lattice has the sphere topology, the model has a unique ground state $|\Phi\rangle$ up to scalar factors.

A.1 Topological Features

We briefly review the topological nature of the ground-state subspace of the string-net model defined in Ref. [2]. Topologically, any two lattices with the same topology can be transformed into each other by the *Pachner moves*. There are unitary linear maps between the Hilbert spaces of two string-net models with the same input UFC on different lattices related by the Pachner moves[46], formally denoted as operators \mathcal{T} . The ground states are invariant under such linear transformations. There are three kinds of elementary Pachner moves, whose corresponding linear transformations are:

$$\begin{aligned} \mathcal{T} \begin{array}{c} a \quad d \\ \diagdown \quad / \\ m \\ / \quad \diagdown \\ b \quad c \end{array} &= \sum_{n \in L_{\mathcal{F}}} \sqrt{d_m d_n} G_{cdn}^{abm} \begin{array}{c} a \quad d \\ \diagdown \quad / \\ n \\ / \quad \diagdown \\ b \quad c \end{array}, \\ \mathcal{T} \begin{array}{c} b \\ \uparrow \\ x \quad \times \quad y \\ \downarrow \\ a \end{array} &= \sqrt{\frac{d_x d_y}{d_a}} \delta_{ab} \delta_{xya^*} \begin{array}{c} | \\ a \end{array}, \\ \mathcal{T} \begin{array}{c} | \\ a \end{array} &= \frac{1}{D} \sum_{xy \in L_{\mathcal{F}}} \sqrt{\frac{d_x d_y}{d_a}} \delta_{xya^*} \begin{array}{c} a \\ \uparrow \\ x \quad \times \quad y \\ \downarrow \\ a \end{array}. \end{aligned} \quad (\text{A.4})$$

Here, “ \times ” marks a plaquette to be contracted. These three elementary Pachner moves and their corresponding unitary transformations can be composed. Given initial and final lattices, there are multiple ways to compose these elementary Pachner moves, but different ways result in the same transformation matrices on the ground-state Hilbert space.

We have also noted that for a plaquette, different choices of edge to which the tail is attached are equivalent. These variations lead to distinct lattice configurations and, consequently, different Hilbert spaces for the lattice model. The equivalence between such two Hilbert spaces is established by the following linear transformation \mathcal{T}' :

$$\mathcal{T}' \begin{array}{c} \downarrow \\ \downarrow \\ e_1 \quad i_2 \\ \diagdown \quad / \\ i_1 \quad p \\ / \quad \diagdown \\ i_0 \end{array} = \sum_{j \in L_{\mathcal{F}}} \sqrt{d_{i_1} d_j} G_{i_0 p^* j}^{i_2^* e_1 i_1} \begin{array}{c} \downarrow \\ \downarrow \\ e_1 \quad j \quad i_2 \\ \diagdown \quad / \quad \diagdown \quad / \\ i_0 \quad p \\ / \quad \diagdown \\ e_n \quad i_n \\ \downarrow \end{array}. \quad (\text{A.5})$$

The states where tails attach to other edges can be obtained recursively in this manner.

For convenience, in certain cases, we will temporarily incorporate auxiliary states with multiple tails within a single plaquette. These states, despite having multiple tails in one plaquette, are all equivalent to states within the Hilbert space (with only one tail in each plaquette):

$$= \sum_{u \in L_{\mathcal{F}}} \sqrt{d_j d_p} G_{i_0 s^* p}^{r^* i_1^* j} \quad (A.6)$$

A.2 Excited States

An *excited state* $|\varphi\rangle$ of the string-net model is an eigenstate such that $Q_P|\varphi\rangle = 0$ at some plaquettes P . In such a state, we say there are *anyons* in these plaquettes P . We also refer to the ground states as trivial excited states, in which there are only *trivial anyons* in all plaquettes. We assume the sphere topology, in which the model has a unique ground state; nevertheless, the results in this section apply to other topologies.

We start with the simplest excited states with a pair of anyons in two *adjacent* plaquettes with a common edge E . This state can be generated by ribbon operator $W_E^{J;pq}$, which is a composition of an auxiliary operator $\mathcal{W}_E^{J;pq}$

$$\mathcal{W}_E^{J;pq} \left| j \right\rangle := \sum_{k \in L_{\mathcal{F}}} \sqrt{\frac{d_k}{d_{j_E}}} z_{pqj_E}^{J;k} \quad (A.7)$$

and Pachner moves (A.5) and (A.6), where j_E is the dof on edge E . For any state in the Hilbert space of the model, each plaquette contains exactly one tail attached to a specific edge (could be edge E) of the plaquette. Operator $\mathcal{W}_E^{J;pq}$ (A.7) introduces two new tails on edge E , and these new tails must be moved and fused with the original tails of the plaquettes by the subsequent Pachner moves in the creation operator.

The coefficients in Eq. (A.7), $z_{pqj}^{J;k}$, are called the *half-braiding tensor* of anyon type J , defined by the following equation:

$$\frac{\delta_{jt} N_{rs}^t}{d_t} z_{pqt}^{J;w} = \sum_{u, l, v \in L_{\mathcal{F}}} z_{lqr}^{J;v} z_{pls}^{J;u} d_u d_v G_{p^* w u^*}^{r^* s^* t} G_{q w^* v}^{s r j^*} G_{r v^* w}^{s^* u l^*}. \quad (A.8)$$

We will discuss the physical significance of this equation in Appendix A.3. The label J , called the *anyon type*, labels different minimal solutions z^J of Eq. (A.8) that cannot be the sum of any other nonzero solutions. Categorically, anyon type J are labeled by simple objects in the *center* of UFC \mathcal{F} , a modular tensor category whose categorical data record all topological properties of the topological order that the string-net model describes, denoted as $\mathcal{Z}(\mathcal{F})$. In particular, the trivial anyon $\mathcal{J} \in L_{\mathcal{Z}(\mathcal{F})}$ satisfies

$$z_{pqj}^{\mathcal{J};k} = \delta_{p1} \delta_{q1} \delta_{jk}.$$

The statistics of anyon J are recorded by the diagonal element of modular T matrix of UMTC $\mathcal{Z}(\mathcal{F})$, where

$$T_{JK} = \frac{1}{d_t} \delta_{JK} \sum_{p \in L_{\mathcal{F}}} d_p z_{ttt}^{J;p}.$$

Here, t is an arbitrary charge of anyon J . The braiding of two anyons J and K is recorded by the modular S matrix, whose matrix elements are

$$S_{JK} = \frac{1}{D} \sum_{p,q,k \in L_{\mathcal{F}}} d_k \bar{z}_{ppq}^{J;k} \bar{z}_{qqp}^{K;k}.$$

An anyon J has trivial self-statistics if $\theta_J = 1$; two anyons J and K braid trivially if and only if $S_{JK} = d_J d_K$, where d_J is the quantum dimension of anyon J , defined as

$$d_J = \sum_{J \text{ Charges } p} d_p.$$

States with two quasiparticles in two non-adjacent plaquettes are generated by ribbon operators along longer paths. These longer ribbon operators result from concatenating shorter ribbon operators. For example, to create two quasiparticles J^* and J with charges p_0^* and p_n in two non-adjacent plaquettes P_0 and P_n , we can choose a sequence of plaquettes (P_0, P_1, \dots, P_n) , where P_i and P_{i+1} are adjacent plaquettes with their common edge E_i . The ribbon operator $W_{P_0 P_n}^{J;p_0 p_n}$ is

$$W_{P_0 P_n}^{J;p_0 p_n} := \left[\sum_{p_1 p_2 \dots p_{n-1} \in L_{\mathcal{F}}} \prod_{k=1}^{n-1} \left(d_{p_k} B_{P_k} W_{E_k}^{J;p_k p_{k+1}} \right) \right] W_{E_0}^{J;p_0 p_1}.$$

Different choices of plaquette paths (P_0, P_1, \dots, P_n) give the same operator $W_{P_0 P_n}^{J;p_0 p_n}$ if these sequences can deform continuously from one to another. Following the same procedure, we can also define the creation operator of three or more anyons.

At the end of this section, we define the measurement operator M_P^J measuring whether there is an anyon J excited in plaquette P :

$$M_P^J := \sum_{s,t \in L_{\mathcal{F}}} \frac{d_s d_t z_{pps}^{J;t}}{d_p} \cdot \quad (\text{A.9})$$

The set of measurement operators are orthonormal and complete:

$$M_P^J M_P^K = \delta_{JK} M_P^J, \quad \sum_{J \in L_{\mathcal{Z}}(\mathcal{F})} M_P^J = \mathbf{1}.$$

A.3 The Output UMTC is the Center of the Input UFC

As mentioned earlier, the string-net model's output UMTC $\mathcal{Z}(\mathcal{F})$ is the center of its input UFC \mathcal{F} , and the model is a physical representation of this center relationship. In this appendix, we explicitly demonstrate how this representation is understood.

Categorically, an object J in the center $\mathcal{Z}(\mathcal{F})$ is denoted as a pair $J = (X_J, c_{X_J, \cdot})$, where X_J is an object in UFC \mathcal{F} , and $c_{X_J, \cdot}$, called a *half-braiding*, is a set of morphisms

$$\{c_{X_J, y} : X_J \otimes y \rightarrow y \otimes X_J | y \in \mathcal{F}\}.$$

A morphism $c_{X_J, y}$ braids object X_J with object y in \mathcal{F} and can be depicted as

In a UFC, all morphisms can be decomposed as direct sums of fusion of simple objects, and so can a half-braiding:

$$\text{crossing} = \bigoplus_{p, q \in L_J} \bigoplus_{k \in L_{\mathcal{F}}} \sqrt{\frac{d_k}{d_y}} z_{pqy}^{J;k} \text{fusion diagram} . \quad (\text{A.10})$$

Here, $L_J \subseteq L_{\mathcal{F}}$, such that the direct sum of simple objects in L_J is X_J :

$$X_J = \bigoplus_{p \in L_J} p.$$

The expansion coefficients $z_{pqk}^{J;y}$ are known as the *half-braiding tensor* of J . A half-braiding should commute with any fusion in \mathcal{F} :

$$\text{fusion then half-braiding} = \text{half-braiding then fusion} . \quad (\text{A.11})$$

Expanding Eqs. (A.11) using Eq. (A.10) leads to Eq. (A.8).

For a string-net model with input UFC \mathcal{F} , an anyon type J is a simple object in the output UMTC $\mathcal{Z}(\mathcal{F})$, and J 's charges take value in L_J . The action of creation operator $W_E^{J;pq}$ directly represents the half-braiding morphism c_{X_J, j_E} of object X_J with $j_E \in L_{\mathcal{F}}$, the dof on edge E :

$$\text{crossing} = \sum_{k \in L_{\mathcal{F}}} \sqrt{\frac{d_k}{d_{j_E}}} z_{pqj_E}^{J;k} \text{fusion diagram} = W_E^{J;pq} |j_E\rangle .$$

The simplest creation operator $W_E^{J;(p,\alpha)(q,\beta)}$ creating a pair of dyons (J^*, p^*, α) and (J, q, β) in two adjacent plaquettes separated by edge E is now defined as

$$W_E^{J;(p,\alpha)(q,\beta)} \begin{array}{c} e_1 \quad i_2 \\ \swarrow \quad \searrow \\ j \\ \swarrow \quad \searrow \\ 1_{J,1} \quad j \\ \swarrow \quad \searrow \\ e_n \quad i_n \end{array} := \sum_{k \in L_{\mathcal{F}}} \sqrt{\frac{d_k}{d_j}} \overline{[z_{pqj}^{J;k}]_{\alpha\beta}} \begin{array}{c} e_1 \quad i_2 \\ \swarrow \quad \searrow \\ j \\ \swarrow \quad \searrow \\ p_{J^*,\alpha} \quad k \\ \swarrow \quad \searrow \\ e_n \quad i_n \end{array}, \quad (\text{A.12})$$

Here, $J \in L_{\mathcal{Z}(\mathcal{F})}$ is the trivial anyon with unique charge $1 \in L_{\mathcal{F}}$ and has no degeneracy $n_J = 1$. The creation operator multiplications depend on the CG coefficients of the tensor products of the half-braiding z -tensors. We will not detail them here.

A typical example of such a non-commutative input UFC is $\text{Vec}(G)$, where G is a nonabelian group. The simple objects of UFC $\text{Vec}(G)$ are labeled by group elements in G , and for any $a, b, c, d, e, f \in G$,

$$\delta_{abc} = 1 \quad \text{if } c^* = ab \quad \text{else } 0, \quad d_a = 1, \quad G_{cdf}^{abe} = \delta_{abe} \delta_{bcf^*} \delta_{cde^*} \delta_{daf},$$

where c^* is the inversed element of $c \in G$. Equation (A.8) for z -tensors turns out to be

$$z_{p(a^*pa)a}^{J;(pa)} z_{(a^*pa)(b^*a^*pab)b}^{J;(a^*pab)} = z_{p(b^*a^*pab)(ab)}^{J;(pab)}.$$

Consequently, the anyon types J are labeled by a pair

$$J = (\bar{p}, \rho),$$

where $\bar{p} = \{g^*pg | g \in G\}$ for $p \in G$ is a conjugate class of G containing element p , and ρ is an irreducible representation of the centralizer of conjugate class \bar{p} :

$$Z(\bar{p}) = \{g \in G | g^*pg = p\}.$$

The multiplet degeneracy of each dyon multiplet (J, p) of anyon type J is the dimension of irrep ρ of centralizer $Z(\bar{p})$:

$$n_{((\bar{p}, \rho), p)} = \dim \rho,$$

and the quantum dimension of anyon J is $n_{((\bar{p}, \rho), p)} |\bar{p}|$, the number of all J 's local dofs.

In particular, the fluxons in the string-net model with input UFC $\text{Vec}G$ are those dyons with anyon type $(\bar{1}, \rho)$, whose trivial conjugate class is $\bar{1} = \{1\} \subset G$ and $Z(\bar{1}) = G$. The corresponding half-braiding tensor is:

$$z_{1,1,r}^{(\bar{1}, \rho); r} = D_{\alpha\beta}^\rho(g), \quad 1 \leq \alpha, \beta \leq \dim \rho, \quad \forall r \in G.$$

where D^ρ is the representation matrix of irrep ρ of group G .

B The Anyon Species of S_3 Quantum Double Phase

There are 8 types of anyons in $D(S_3)$ phase, which is showed in Table 1.

Their corresponding z -tensors are:

$$z_{1,1,1}^{A;1} = z_{1,1,r}^{A;r} = z_{1,1,r^2}^{A;r^2} = z_{1,1,s}^{A;s} = z_{1,1,rs}^{A;rs} = z_{1,1,sr}^{A;sr} = 1; \quad (\text{B.1})$$

$$z_{1,1,1}^{B;1} = z_{1,1,r}^{B;r} = z_{1,1,r^2}^{B;r^2} = 1, \quad z_{1,1,s}^{B;s} = z_{1,1,rs}^{B;rs} = z_{1,1,sr}^{B;sr} = -1; \quad (\text{B.2})$$

$$\begin{aligned} z_{1,1,1,1}^{C;1} &= 1, \quad z_{1,1,1,r}^{C;r} = e^{i\frac{2\pi}{3}}, \quad z_{1,1,1,r^2}^{C;r^2} = e^{-i\frac{2\pi}{3}}, \\ z_{1,2,1,1}^{C;1} &= 1, \quad z_{1,2,1,2,r}^{C;r} = e^{-i\frac{2\pi}{3}}, \quad z_{1,2,1,2,r^2}^{C;r^2} = e^{i\frac{2\pi}{3}}, \\ z_{1,1,1,2,s}^{C;s} &= 1, \quad z_{1,1,1,2,rs}^{C;rs} = e^{i\frac{2\pi}{3}}, \quad z_{1,1,1,2,sr}^{C;sr} = e^{-i\frac{2\pi}{3}}, \\ z_{1,2,1,1,s}^{C;s} &= 1, \quad z_{1,2,1,1,rs}^{C;rs} = e^{-i\frac{2\pi}{3}}, \quad z_{1,2,1,1,sr}^{C;sr} = e^{i\frac{2\pi}{3}}; \end{aligned} \quad (\text{B.3})$$

$$\begin{aligned} z_{s,s,1}^{D;s} &= z_{s,rs,r}^{D;sr} = z_{s,rs,r^2}^{D;rs} = z_{rs,rs,1}^{D;rs} = z_{rs,rs,r}^{D;s} = z_{rs,s,r^2}^{D;sr} = 1, \\ z_{sr,rs,1}^{D;sr} &= z_{sr,s,r}^{D;rs} = z_{sr,rs,r^2}^{D;s} = z_{s,s,s}^{D;1} = z_{s,rs,rs}^{D;r} = z_{s,rs,rs}^{D;r^2} = 1, \\ z_{rs,rs,rs}^{D;1} &= z_{rs,rs,s}^{D;r} = z_{rs,s,rs}^{D;r^2} = z_{sr,rs,rs}^{D;1} = z_{sr,s,rs}^{D;r} = z_{sr,rs,s}^{D;r^2} = 1; \end{aligned} \quad (\text{B.4})$$

$$\begin{aligned} z_{s,s,1}^{E;s} &= z_{s,rs,r}^{E;sr} = z_{s,rs,r^2}^{E;rs} = z_{rs,rs,1}^{E;rs} = z_{rs,rs,r}^{E;s} = z_{rs,s,r^2}^{E;sr} = 1, \\ z_{sr,rs,1}^{E;sr} &= z_{sr,s,r}^{E;rs} = z_{sr,rs,r^2}^{E;s} = 1, \quad z_{s,s,s}^{E;1} = z_{s,rs,rs}^{E;r} = z_{s,rs,rs}^{E;r^2} = -1, \\ z_{rs,rs,rs}^{E;1} &= z_{rs,rs,s}^{E;r} = z_{rs,s,rs}^{E;r^2} = z_{sr,rs,rs}^{E;1} = z_{sr,s,rs}^{E;r} = z_{sr,rs,s}^{E;r^2} = -1; \end{aligned} \quad (\text{B.5})$$

$$\begin{aligned} z_{r,r,1}^{F;r} &= z_{r,r,r}^{F;r^2} = z_{r,r,r^2}^{F;1} = z_{r^2,r^2,1}^{F;r^2} = z_{r^2,r^2,r}^{F;1} = z_{r^2,r^2,r^2}^{F;r} = 1, \\ z_{r,r^2,s}^{F;rs} &= z_{r,r^2,rs}^{F;sr} = z_{r,r^2,rs}^{F;rs} = z_{r^2,r,s}^{F;sr} = z_{r^2,r,rs}^{F;s} = z_{r^2,r,rs}^{F;rs} = 1; \end{aligned} \quad (\text{B.6})$$

$$\begin{aligned} z_{r,r,1}^{G;r} &= 1, \quad z_{r,r,r}^{G;r^2} = e^{i\frac{2\pi}{3}}, \quad z_{r,r,r^2}^{G;1} = e^{-i\frac{2\pi}{3}}, \\ z_{r^2,r^2,1}^{G;r^2} &= 1, \quad z_{r^2,r^2,r}^{G;1} = e^{-i\frac{2\pi}{3}}, \quad z_{r^2,r^2,r^2}^{G;r} = e^{i\frac{2\pi}{3}}, \\ z_{r,r^2,s}^{G;rs} &= 1, \quad z_{r,r^2,rs}^{G;sr} = e^{i\frac{2\pi}{3}}, \quad z_{r,r^2,rs}^{G;rs} = e^{-i\frac{2\pi}{3}}, \\ z_{r^2,r,s}^{G;sr} &= 1, \quad z_{r^2,r,rs}^{G;s} = e^{-i\frac{2\pi}{3}}, \quad z_{r^2,r,rs}^{G;rs} = e^{i\frac{2\pi}{3}}; \end{aligned} \quad (\text{B.7})$$

$$\begin{aligned} z_{r,r,1}^{H;r} &= 1, \quad z_{r,r,r}^{H;r^2} = e^{-i\frac{2\pi}{3}}, \quad z_{r,r,r^2}^{H;1} = e^{i\frac{2\pi}{3}}, \\ z_{r^2,r^2,1}^{H;r^2} &= 1, \quad z_{r^2,r^2,r}^{H;1} = e^{i\frac{2\pi}{3}}, \quad z_{r^2,r^2,r^2}^{H;r} = e^{-i\frac{2\pi}{3}}, \\ z_{r,r^2,s}^{H;rs} &= 1, \quad z_{r,r^2,rs}^{H;sr} = e^{-i\frac{2\pi}{3}}, \quad z_{r,r^2,rs}^{H;rs} = e^{i\frac{2\pi}{3}}, \\ z_{r^2,r,s}^{H;sr} &= 1, \quad z_{r^2,r,rs}^{H;s} = e^{i\frac{2\pi}{3}}, \quad z_{r^2,r,rs}^{H;rs} = e^{-i\frac{2\pi}{3}}. \end{aligned} \quad (\text{B.8})$$

C Multi-fusion Category as the Input of SET Model

In this section, we introduce how the multifusion category can be used as the input of SET string-net model.

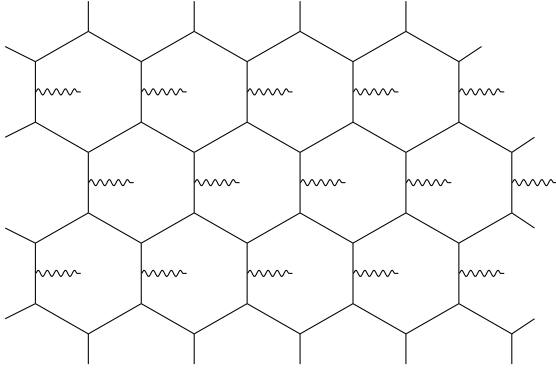


Figure 6: The lattice of HGW model.

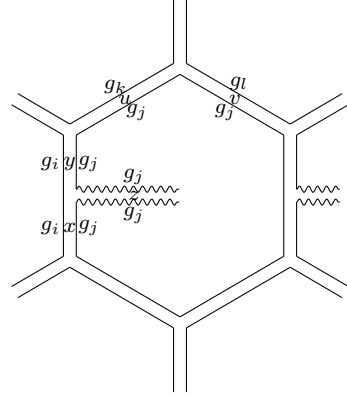


Figure 7: The fattened lattice of one plaquette.

C.1 Input data: A Multifusion Category with Associated Isomorphisms

When a topological phase \mathcal{C} is paired with a global symmetry G , it becomes an SET phase, denoted as \mathcal{C}_G . The SET phase \mathcal{C}_G comprises multiple G -graded sectors, each of which is topologically equivalent to \mathcal{C} but distinguished by a unique element from the symmetry group. The action of G facilitates transitions between these G -graded sectors. This observation leads to the development of a lattice model for \mathcal{C}_G by iterating the HGW string-net model of \mathcal{C} a corresponding number of times. These iterations are interconnected through the elements of the group G , ensuring that in any basis configuration of the string-net model, each plaquette is associated with a specific G -graded sector. Given that the input data for the HGW model of phase \mathcal{C} is a UFC \mathcal{F} , it follows that the input data for the lattice model associated with the \mathcal{C}_G phase should similarly involve a proportional number of \mathcal{F} copies, which are interconnected via the symmetry G . This configuration is mathematically formalized as a multifusion category \mathcal{M} endowed with a G -action.

To grasp the concept of a multifusion category, consider a straightforward example where a multifusion category \mathcal{M} , derived from an \mathcal{F} , is generally expressed in matrix form:

$$\mathcal{M} = \begin{pmatrix} \mathcal{F}_{g_1 g_1} & \mathcal{F}_{g_1 g_2} & \cdots & \mathcal{F}_{g_1 g_n} \\ \mathcal{F}_{g_2 g_1} & \mathcal{F}_{g_2 g_2} & \cdots & \mathcal{F}_{g_2 g_n} \\ \vdots & \vdots & \ddots & \vdots \\ \mathcal{F}_{g_n g_1} & \mathcal{F}_{g_n g_2} & \cdots & \mathcal{F}_{g_n g_n} \end{pmatrix}, \quad (\text{C.1})$$

Each $\mathcal{F}_{g_i g_j}$ can be considered as an instance of \mathcal{F} when viewed as a UFC. Generally, the size n corresponds to $|G|$, considering G is finite. A simple object within \mathcal{M} is symbolized by $x_{g_i g_j}$, which also represents a simple object within $\mathcal{F}_{g_i g_j}$, where x is a simple object within \mathcal{F} . These simple objects adhere to the subsequent fusion rules:

$$x_{g_i g_j} \otimes y_{g_k g_l} = \begin{cases} (x \otimes y)_{g_i g_l} & (g_j = g_k), \\ 0 & (g_j \neq g_k) \end{cases}, \quad (\text{C.2})$$

where \mathbb{O} is the zero object of \mathcal{M} , and $x \otimes y$ is a fusion in \mathcal{F} .

According to the fusion rules, the lattice illustrated in Figure 6 can be expanded by transforming each edge or tail into a double line, whereby the indices of the group elements reside on the double lines [16], as shown in Figure 7. It is evident that each plaquette can now be uniquely identified by a group element g , with g serving as the label for the loop of the inner-side line within the respective plaquette. We refer to the plaquette as being in a g -sector. This method is equivalent to introducing spins into the plaquettes [17].

The simple objects corresponding to the diagonal elements \mathcal{F}_{gg} of the multifusion matrix (C.1) characterize the degrees of freedom (dofs) in sector- g . In contrast, the simple objects associated with the off-diagonal elements characterize the domain wall degrees of freedom. Specifically, the simple objects within $\mathcal{F}_{g_i g_j}$ describe the domain wall between sector- g_i and sector- g_j .

Considering the structure of the input data, the lattice configuration of our SET model for phase \mathcal{C}_G mirrors precisely that of the HGW string-net model for phase \mathcal{C} . This lattice is a honeycomb arrangement, where each plaquette is represented with a tail (a wiggly dangling edge), as depicted in Figure 6. Each edge and tail of the lattice embodies a degree of freedom that assumes values from the simple objects of \mathcal{M} , thereby ensuring that the fusion rules of M are satisfied at every vertex within the lattice.

C.2 Hamiltonian

The Hamiltonian takes the form

$$H = - \sum_p Q_p = - \sum_p \sum_s Q_p^s, \quad (\text{C.3})$$

where p represents a summation over all plaquettes and s encompasses all simple objects in the multifusion category \mathcal{M} . The Hamiltonian here is identical to the one described in Ref. [7], which provides a reformulation of the Hamiltonian for the HGW string-net model, ensuring uniform energy levels for all elementary anyon excitations. The operators Q_p^s are discussed in detail in Appendix A.

While Hamiltonian (C.3) theoretically aligns with the HGW string-net model representing a pure topological phase, the physical phenomena it represents diverges notably from that of the HGW model. Specifically, the system incorporates both anyon excitations, known as anyons, and local excitations, which the HGW model lacks. In the Symmetry-Enriched Topological (SET) phase characterized by Hamiltonian (C.3), the anyon excitations are defined in respect to the local excitations, which should be considered as part of the vacuum. This phenomenon, referred to as symmetry fractionalization, arises due to the nontrivial action of global symmetry on the topological vacuum, which includes local excitations. Consequently, this interaction results in distinct sectors graded by the symmetry group G . Through the fusion rules of anyons, specific types of anyons are permitted to reside within a G -graded sector where they carry fractionalized symmetry charges. It is important to note that the ground-state degeneracy of a symmetry-enriched topological (SET) phase, denoted as \mathcal{C}_G , remains equivalent to that of the purely topological phase \mathcal{C} for any given topology, notwithstanding the presence of G -graded sectors.

D The Categorical Data of \mathbb{Z}_2 Symmetry Enriched S_3 Multi-fusion Category

The input multifusion category of \mathbb{Z}_2 symmetry enriched S_3 string-net model can be represented by the multifusion matrix

$$\mathcal{M} = \begin{pmatrix} \{1_{++}, r_{++}, r_{++}^2, s_{++}, rs_{++}, sr_{++}\} & \{\alpha_{+-}, \beta_{+-}\} \\ \{\alpha_{-+}, \beta_{-+}\} & \{1_{--}, r_{--}, r_{--}^2, s_{--}, rs_{--}, sr_{--}\} \end{pmatrix}. \quad (\text{D.1})$$

In this section, we will list the categorical data of this multifusion category.

D.1 The Fusion Rules

The fusion rules are

$$\begin{aligned} \delta_{M_K M_L M_N} &= \delta_{klm}, \quad \forall M_K, M_L, M_N \in \{1_{--}, r_{++}, r_{++}^2, s_{++}, rs_{++}, sr_{++}\}, \\ \delta_{\alpha_{-+} 1_{++} \alpha_{+-}} &= \delta_{\alpha_{-+} r_{++} \alpha_{+-}} = \delta_{\alpha_{-+} r_{++}^2 \alpha_{+-}} = \delta_{\beta_{-+} 1_{++} \beta_{+-}} = \delta_{\beta_{-+} r_{++} \beta_{+-}} = \delta_{\beta_{-+} r_{++}^2 \beta_{+-}} = 1, \\ \delta_{\alpha_{-+} s_{++} \beta_{+-}} &= \delta_{\alpha_{-+} rs_{++} \beta_{+-}} = \delta_{\alpha_{-+} sr_{++} \beta_{+-}} = \delta_{\beta_{-+} s_{++} \alpha_{+-}} = \delta_{\beta_{-+} rs_{++} \alpha_{+-}} = \delta_{\beta_{-+} sr_{++} \alpha_{+-}} = 1, \\ \delta_{\alpha_{-+} \alpha_{+-} 1_{--}} &= \delta_{\alpha_{-+} \alpha_{+-} r_{--}} = \delta_{\alpha_{-+} \alpha_{+-} r_{--}^2} = \delta_{\beta_{-+} \beta_{+-} 1_{--}} = \delta_{\beta_{-+} \beta_{+-} r_{--}} = \delta_{\beta_{-+} \beta_{+-} r_{--}^2} = 1, \\ \delta_{\alpha_{-+} \beta_{+-} s_{--}} &= \delta_{\alpha_{-+} \beta_{+-} rs_{--}} = \delta_{\alpha_{-+} \beta_{+-} sr_{--}} = \delta_{\beta_{-+} \alpha_{+-} s_{--}} = \delta_{\beta_{-+} \alpha_{+-} rs_{--}} = \delta_{\beta_{-+} \alpha_{+-} sr_{--}} = 1. \end{aligned} \quad (\text{D.2})$$

D.2 The $6j$ -Symbols

The non-zero $6j$ -symbols are

$$\begin{aligned} G_{\alpha_{+-} \alpha_{+-} 1_{--}}^{\alpha_{+-} \alpha_{+-} 1_{++}} &= G_{\alpha_{+-} \alpha_{+-} r_{--}}^{\alpha_{+-} \alpha_{+-} 1_{++}} = G_{\alpha_{+-} \alpha_{+-} r_{--}^2}^{\alpha_{+-} \alpha_{+-} 1_{++}} = \frac{1}{\sqrt{3}}, \\ G_{\alpha_{+-} \alpha_{+-} 1_{--}}^{\alpha_{+-} \alpha_{+-} r_{++}} &= \frac{1}{\sqrt{3}}, \quad G_{\alpha_{+-} \alpha_{+-} r_{--}}^{\alpha_{+-} \alpha_{+-} r_{++}} = \frac{e^{-i\frac{2\pi}{3}}}{\sqrt{3}}, \quad G_{\alpha_{+-} \alpha_{+-} r_{--}^2}^{\alpha_{+-} \alpha_{+-} r_{++}} = \frac{e^{i\frac{2\pi}{3}}}{\sqrt{3}}, \\ G_{\alpha_{+-} \alpha_{+-} 1_{--}}^{\alpha_{+-} \alpha_{+-} r_{++}^2} &= \frac{1}{\sqrt{3}}, \quad G_{\alpha_{+-} \alpha_{+-} r_{--}}^{\alpha_{+-} \alpha_{+-} r_{++}^2} = \frac{e^{i\frac{2\pi}{3}}}{\sqrt{3}}, \quad G_{\alpha_{+-} \alpha_{+-} r_{--}^2}^{\alpha_{+-} \alpha_{+-} r_{++}^2} = \frac{e^{-i\frac{2\pi}{3}}}{\sqrt{3}}, \\ G_{\beta_{+-} \beta_{+-} 1_{--}}^{\beta_{+-} \beta_{+-} 1_{++}} &= G_{\beta_{+-} \beta_{+-} r_{--}}^{\beta_{+-} \beta_{+-} 1_{++}} = G_{\beta_{+-} \beta_{+-} r_{--}^2}^{\beta_{+-} \beta_{+-} 1_{++}} = \frac{1}{\sqrt{3}}, \\ G_{\beta_{+-} \beta_{+-} 1_{--}}^{\beta_{+-} \beta_{+-} r_{++}} &= \frac{1}{\sqrt{3}}, \quad G_{\beta_{+-} \beta_{+-} r_{--}}^{\beta_{+-} \beta_{+-} r_{++}} = \frac{e^{i\frac{2\pi}{3}}}{\sqrt{3}}, \quad G_{\beta_{+-} \beta_{+-} r_{--}^2}^{\beta_{+-} \beta_{+-} r_{++}} = \frac{e^{-i\frac{2\pi}{3}}}{\sqrt{3}}, \\ G_{\beta_{+-} \beta_{+-} 1_{--}}^{\beta_{+-} \beta_{+-} r_{++}^2} &= \frac{1}{\sqrt{3}}, \quad G_{\beta_{+-} \beta_{+-} r_{--}}^{\beta_{+-} \beta_{+-} r_{++}^2} = \frac{e^{-i\frac{2\pi}{3}}}{\sqrt{3}}, \quad G_{\beta_{+-} \beta_{+-} r_{--}^2}^{\beta_{+-} \beta_{+-} r_{++}^2} = \frac{e^{i\frac{2\pi}{3}}}{\sqrt{3}}, \\ G_{\beta_{+-} \alpha_{+-} 1_{--}}^{\alpha_{+-} \beta_{+-} s_{++}} &= G_{\beta_{+-} \alpha_{+-} r_{--}}^{\alpha_{+-} \beta_{+-} s_{++}} = G_{\beta_{+-} \alpha_{+-} r_{--}^2}^{\alpha_{+-} \beta_{+-} s_{++}} = \frac{1}{\sqrt{3}}, \\ G_{\beta_{+-} \alpha_{+-} 1_{--}}^{\alpha_{+-} \beta_{+-} rs_{++}} &= \frac{1}{\sqrt{3}}, \quad G_{\beta_{+-} \alpha_{+-} r_{--}}^{\alpha_{+-} \beta_{+-} rs_{++}} = \frac{e^{i\frac{2\pi}{3}}}{\sqrt{3}}, \quad G_{\beta_{+-} \alpha_{+-} r_{--}^2}^{\alpha_{+-} \beta_{+-} rs_{++}} = \frac{e^{-i\frac{2\pi}{3}}}{\sqrt{3}}, \end{aligned}$$

$$\begin{aligned}
G_{\beta_+-\alpha_++1--}^{\alpha_+-\beta_++sr++} &= \frac{1}{\sqrt{3}}, \quad G_{\beta_+-\alpha_++r--}^{\alpha_+-\beta_++sr++} = \frac{e^{-i\frac{2\pi}{3}}}{\sqrt{3}}, \quad G_{\beta_+-\alpha_++r_{--}^2}^{\alpha_+-\beta_++sr++} = \frac{e^{i\frac{2\pi}{3}}}{\sqrt{3}}, \\
G_{\beta_+-\beta_++s--}^{\alpha_+-\alpha_++1++} &= G_{\beta_+-\beta_++rs--}^{\alpha_+-\alpha_++1++} = G_{\beta_+-\beta_++sr--}^{\alpha_+-\alpha_++1++} = \frac{1}{\sqrt{3}}, \\
G_{\beta_+-\beta_++s--}^{\alpha_+-\alpha_++r++} &= \frac{1}{\sqrt{3}}, \quad G_{\beta_+-\beta_++rs--}^{\alpha_+-\alpha_++r++} = \frac{e^{-i\frac{2\pi}{3}}}{\sqrt{3}}, \quad G_{\beta_+-\beta_++sr--}^{\alpha_+-\alpha_++r++} = \frac{e^{i\frac{2\pi}{3}}}{\sqrt{3}}, \\
G_{\beta_+-\beta_++s--}^{\alpha_+-\alpha_++r_{++}^2} &= \frac{1}{\sqrt{3}}, \quad G_{\beta_+-\beta_++rs--}^{\alpha_+-\alpha_++r_{++}^2} = \frac{e^{i\frac{2\pi}{3}}}{\sqrt{3}}, \quad G_{\beta_+-\beta_++sr--}^{\alpha_+-\alpha_++r_{++}^2} = \frac{e^{-i\frac{2\pi}{3}}}{\sqrt{3}}, \\
G_{\alpha_+-\beta_++s--}^{\alpha_+-\beta_++s++} &= G_{\alpha_+-\beta_++rs--}^{\alpha_+-\beta_++s++} = G_{\alpha_+-\beta_++sr--}^{\alpha_+-\beta_++s++} = \frac{1}{\sqrt{3}}, \\
G_{\alpha_+-\beta_++s--}^{\alpha_+-\beta_++rs++} &= \frac{1}{\sqrt{3}}, \quad G_{\alpha_+-\beta_++rs--}^{\alpha_+-\beta_++rs++} = \frac{e^{i\frac{2\pi}{3}}}{\sqrt{3}}, \quad G_{\alpha_+-\beta_++sr--}^{\alpha_+-\beta_++rs++} = \frac{e^{-i\frac{2\pi}{3}}}{\sqrt{3}}, \\
G_{\alpha_+-\beta_++s--}^{\alpha_+-\beta_++sr++} &= \frac{1}{\sqrt{3}}, \quad G_{\alpha_+-\beta_++rs--}^{\alpha_+-\beta_++sr++} = \frac{e^{-i\frac{2\pi}{3}}}{\sqrt{3}}, \quad G_{\alpha_+-\beta_++sr--}^{\alpha_+-\beta_++sr++} = \frac{e^{i\frac{2\pi}{3}}}{\sqrt{3}}, \\
G_{\mu\nu^*\gamma^*}^{abc} &= \frac{1}{4\sqrt{3}}\delta_{abc}\delta_{\nu^*c\mu}\delta_{\gamma^*a\nu}\delta_{\mu^*b\gamma}, \\
\forall a, b, c \in \{1_{++}, r_{++}, r_{++}^2, s_{++}, rs_{++}, sr_{++}\}, \quad \mu, \nu, \gamma \in \{\alpha_+-, \beta_+-\}, \\
G_{\mu^*\nu\gamma}^{abc} &= \frac{1}{4\sqrt{3}}\delta_{abc}\delta_{\nu c\mu^*}\delta_{\gamma a\nu^*}\delta_{\mu b\gamma^*}, \\
\forall a, b, c \in \{1_{--}, r_{--}, r_{--}^2, s_{--}, rs_{--}, sr_{--}\}, \quad \mu, \nu, \gamma \in \{\alpha_+-, \beta_+-\}.
\end{aligned}$$

E The anyon Spectrum of EM-Exchange Symmetry Enriched S_3 String-net Model

In this section, we provide the topological excitation spectrum of EM-exchange symmetry enriched S_3 string-net model. There are 8 kinds of anyon excitations, each one can be denoted by a pair (X, Y) , which means that it appears as the original $D(S_3)$ X -type (Y -type) anyon in the $+$ ($-$) sector. The z -tensors of these excitations are:

$$\begin{aligned}
z_{1_{++}, 1_{++}, 1_{++}}^{(A,A); 1_{++}} &= z_{1_{++}, 1_{++}, r_{++}}^{(A,A); r_{++}} = z_{1_{++}, 1_{++}, r_{++}^2}^{(A,A); r_{++}^2} = z_{1_{++}, 1_{++}, s_{++}}^{(A,A); s_{++}} = 1, \\
z_{1_{++}, 1_{++}, rs_{++}}^{(A,A); rs_{++}} &= z_{1_{++}, 1_{++}, sr_{++}}^{(A,A); sr_{++}} = z_{1_{++}, 1_{--}, \alpha_+-}^{(A,A); \alpha_+-} = z_{1_{++}, 1_{--}, \beta_+-}^{(A,A); \beta_+-} = 1, \\
z_{1_{--}, 1_{--}, 1_{--}}^{(A,A); 1_{--}} &= z_{1_{--}, 1_{--}, r_{--}}^{(A,A); r_{--}} = z_{1_{--}, 1_{--}, r_{--}^2}^{(A,A); r_{--}^2} = z_{1_{--}, 1_{--}, s_{--}}^{(A,A); s_{--}} = 1, \\
z_{1_{--}, 1_{--}, rs_{--}}^{(A,A); rs_{--}} &= z_{1_{--}, 1_{--}, sr_{--}}^{(A,A); sr_{--}} = z_{1_{--}, 1_{++}, \alpha_+-}^{(A,A); \alpha_+-} = z_{1_{--}, 1_{++}, \beta_+-}^{(A,A); \beta_+-} = 1;
\end{aligned}$$

$$\begin{aligned}
z_{1_{++}, 1_{++}, 1_{++}}^{(B,B); 1_{++}} &= z_{1_{++}, 1_{++}, r_{++}}^{(B,B); r_{++}} = z_{1_{++}, 1_{++}, r_{++}^2}^{(B,B); r_{++}^2} = 1, \\
z_{1_{++}, 1_{++}, s_{++}}^{(B,B); s_{++}} &= z_{1_{++}, 1_{++}, rs_{++}}^{(B,B); rs_{++}} = z_{1_{++}, 1_{++}, sr_{++}}^{(B,B); sr_{++}} = -1,
\end{aligned}$$

$$\begin{aligned}
z_{1-- , 1-- , 1--}^{(B,B);1--} &= z_{1-- , 1-- , r_{++}}^{(B,B);r_{++}} = z_{1-- , 1-- , r_{++}^2}^{(B,B);r_{++}^2} = 1, \\
z_{1-- , 1-- , s_{--}}^{(B,B);s_{--}} &= z_{1-- , 1-- , rs_{--}}^{(B,B);rs_{--}} = z_{1-- , 1-- , sr_{--}}^{(B,B);sr_{--}} = -1, \\
z_{1-- , 1-- , \alpha_{+-}}^{(B,B);\alpha_{+-}} &= z_{1-- , 1-- , \beta_{+-}}^{(B,B);\beta_{+-}} = z_{1-- , 1++ , \alpha_{-+}}^{(B,B);\alpha_{-+}} = z_{1-- , 1++ , \beta_{-+}}^{(B,B);\beta_{-+}} = 1;
\end{aligned}$$

$$\begin{aligned}
z_{(11)_{++} , (11)_{++} , 1_{++}}^{(C,F);1_{++}} &= 1, \quad z_{(11)_{++} , (11)_{++} , r_{++}}^{(C,F);r_{++}} = e^{i\frac{2\pi}{3}}, \quad z_{(11)_{++} , (11)_{++} , r_{++}^2}^{(C,F);r_{++}^2} = e^{-i\frac{2\pi}{3}}, \\
z_{(12)_{++} , (12)_{++} , 1_{++}}^{(C,F);1_{++}} &= 1, \quad z_{(12)_{++} , (12)_{++} , r_{++}}^{(C,F);r_{++}} = e^{-i\frac{2\pi}{3}}, \quad z_{(12)_{++} , (12)_{++} , r_{++}^2}^{(C,F);r_{++}^2} = e^{i\frac{2\pi}{3}}, \\
z_{(11)_{++} , (12)_{++} , s_{++}}^{(C,F);s_{++}} &= 1, \quad z_{(11)_{++} , (12)_{++} , rs_{++}}^{(C,F);rs_{++}} = e^{i\frac{2\pi}{3}}, \quad z_{(11)_{++} , (12)_{++} , sr_{++}}^{(C,F);sr_{++}} = e^{-i\frac{2\pi}{3}}, \\
z_{(12)_{++} , (11)_{++} , s_{++}}^{(C,F);s_{++}} &= 1, \quad z_{(12)_{++} , (11)_{++} , rs_{++}}^{(C,F);rs_{++}} = e^{-i\frac{2\pi}{3}}, \quad z_{(12)_{++} , (11)_{++} , sr_{++}}^{(C,F);sr_{++}} = e^{i\frac{2\pi}{3}}, \\
z_{r_{--} , r_{--} , 1_{--}}^{(C,F);r_{--}} &= z_{r_{--} , r_{--} , r_{--}}^{(C,F);r_{--}} = z_{r_{--} , r_{--} , r_{--}^2}^{(C,F);r_{--}} = 1, \\
z_{r_{--}^2 , r_{--}^2 , 1_{--}}^{(C,F);r_{--}^2} &= z_{r_{--}^2 , r_{--}^2 , r_{--}}^{(C,F);1_{--}} = z_{r_{--}^2 , r_{--}^2 , r_{--}^2}^{(C,F);r_{--}} = 1, \\
z_{r_{--} , r_{--}^2 , s_{--}}^{(C,F);rs_{--}} &= z_{r_{--} , r_{--}^2 , rs_{--}}^{(C,F);sr_{--}} = z_{r_{--} , r_{--}^2 , sr_{--}}^{(C,F);rs_{--}} = 1, \\
z_{r_{--}^2 , r_{--} , s_{--}}^{(C,F);sr_{--}} &= z_{r_{--}^2 , r_{--} , rs_{--}}^{(C,F);s_{--}} = z_{r_{--}^2 , r_{--} , sr_{--}}^{(C,F);rs_{--}} = 1, \\
z_{(11)_{++} , r_{--} , \alpha_{+-}}^{(C,F);\alpha_{+-}} &= z_{(12)_{++} , r_{--}^2 , \alpha_{+-}}^{(C,F);\alpha_{+-}} = z_{r_{--} , (11)_{++} , \alpha_{-+}}^{(C,F);\alpha_{-+}} = z_{r_{--}^2 , (12)_{++} , \alpha_{-+}}^{(C,F);\alpha_{-+}} = 1, \\
z_{(11)_{++} , r_{--}^2 , \beta_{+-}}^{(C,F);\beta_{+-}} &= z_{(12)_{++} , r_{--} , \beta_{+-}}^{(C,F);\beta_{+-}} = z_{r_{--}^2 , (11)_{++} , \beta_{-+}}^{(C,F);\beta_{-+}} = z_{r_{--} , (12)_{++} , \beta_{-+}}^{(C,F);\beta_{-+}} = 1;
\end{aligned}$$

$$\begin{aligned}
z_{(11)_{--} , (11)_{--} , 1_{--}}^{(F,C);1_{--}} &= 1, \quad z_{(11)_{--} , (11)_{--} , r_{--}}^{(F,C);r_{--}} = e^{i\frac{2\pi}{3}}, \quad z_{(11)_{--} , (11)_{--} , r_{--}^2}^{(F,C);r_{--}^2} = e^{-i\frac{2\pi}{3}}, \\
z_{(12)_{--} , (12)_{--} , 1_{--}}^{(F,C);1_{--}} &= 1, \quad z_{(12)_{--} , (12)_{--} , r_{--}}^{(F,C);r_{--}} = e^{-i\frac{2\pi}{3}}, \quad z_{(12)_{--} , (12)_{--} , r_{--}^2}^{(F,C);r_{--}^2} = e^{i\frac{2\pi}{3}}, \\
z_{(11)_{--} , (12)_{--} , s_{--}}^{(F,C);s_{--}} &= 1, \quad z_{(11)_{--} , (12)_{--} , rs_{--}}^{(F,C);rs_{--}} = e^{i\frac{2\pi}{3}}, \quad z_{(11)_{--} , (12)_{--} , sr_{--}}^{(F,C);sr_{--}} = e^{-i\frac{2\pi}{3}}, \\
z_{(12)_{--} , (11)_{--} , s_{--}}^{(F,C);s_{--}} &= 1, \quad z_{(12)_{--} , (11)_{--} , rs_{--}}^{(F,C);rs_{--}} = e^{-i\frac{2\pi}{3}}, \quad z_{(12)_{--} , (11)_{--} , sr_{--}}^{(F,C);sr_{--}} = e^{i\frac{2\pi}{3}}, \\
z_{r_{++} , r_{++} , 1_{++}}^{(F,C);r_{++}} &= z_{r_{++} , r_{++} , r_{++}}^{(F,C);r_{++}} = z_{r_{++} , r_{++} , r_{++}^2}^{(F,C);r_{++}} = 1, \\
z_{r_{++}^2 , r_{++}^2 , 1_{++}}^{(F,C);r_{++}^2} &= z_{r_{++}^2 , r_{++}^2 , r_{++}}^{(F,C);1_{++}} = z_{r_{++}^2 , r_{++}^2 , r_{++}^2}^{(F,C);r_{++}} = 1, \\
z_{r_{++} , r_{++}^2 , s_{++}}^{(F,C);rs_{++}} &= z_{r_{++} , r_{++}^2 , rs_{++}}^{(F,C);sr_{++}} = z_{r_{++} , r_{++}^2 , sr_{++}}^{(F,C);rs_{++}} = 1, \\
z_{r_{++}^2 , r_{++} , s_{++}}^{(F,C);sr_{++}} &= z_{r_{++}^2 , r_{++} , rs_{++}}^{(F,C);s_{++}} = z_{r_{++}^2 , r_{++} , sr_{++}}^{(F,C);rs_{++}} = 1, \\
z_{(11)_{--} , r_{++} , \alpha_{-+}}^{(F,C);\alpha_{-+}} &= z_{(12)_{--} , r_{++}^2 , \alpha_{-+}}^{(F,C);\alpha_{-+}} = z_{r_{++} , (11)_{--} , \alpha_{+-}}^{(F,C);\alpha_{+-}} = z_{r_{++}^2 , (12)_{--} , \alpha_{+-}}^{(F,C);\alpha_{+-}} = 1, \\
z_{(11)_{--} , r_{++}^2 , \beta_{-+}}^{(F,C);\beta_{-+}} &= z_{(12)_{--} , r_{++} , \beta_{-+}}^{(F,C);\beta_{-+}} = z_{r_{++}^2 , (11)_{--} , \beta_{+-}}^{(F,C);\beta_{+-}} = z_{r_{++} , (12)_{--} , \beta_{+-}}^{(F,C);\beta_{+-}} = 1;
\end{aligned}$$

$$z_{r_{++} , r_{++} , 1_{++}}^{(G,G);r_{++}} = 1, \quad z_{r_{++} , r_{++} , r_{++}}^{(G,G);r_{++}^2} = e^{i\frac{2\pi}{3}}, \quad z_{r_{++} , r_{++} , r_{++}^2}^{(G,G);1_{++}} = e^{-i\frac{2\pi}{3}},$$

$$\begin{aligned}
z_{r_{++},r_{++},1_{++}}^{(G,G);r_{++}^2} &= 1, \quad z_{r_{++},r_{++},r_{++}}^{(G,G);1_{++}} = e^{-i\frac{2\pi}{3}}, \quad z_{r_{++},r_{++},r_{++}}^{(G,G);r_{++}} = e^{i\frac{2\pi}{3}}, \\
z_{r_{++},r_{++},s_{++}}^{(G,G);rs_{++}} &= 1, \quad z_{r_{++},r_{++},rs_{++}}^{(G,G);sr_{++}} = e^{i\frac{2\pi}{3}}, \quad z_{r_{++},r_{++},sr_{++}}^{(G,G);rs_{++}} = e^{-i\frac{2\pi}{3}}, \\
z_{r_{++},r_{++},s_{++}}^{(G,G);sr_{++}} &= 1, \quad z_{r_{++},r_{++},rs_{++}}^{(G,G);s_{++}} = e^{-i\frac{2\pi}{3}}, \quad z_{r_{++},r_{++},sr_{++}}^{(G,G);rs_{++}} = e^{i\frac{2\pi}{3}}, \\
z_{r_{--},r_{--},1_{--}}^{(G,G);r_{--}^2} &= 1, \quad z_{r_{--},r_{--},r_{--}}^{(G,G);r_{--}^2} = e^{i\frac{2\pi}{3}}, \quad z_{r_{--},r_{--},r_{--}}^{(G,G);1_{--}} = e^{-i\frac{2\pi}{3}}, \\
z_{r_{--},r_{--},1_{--}}^{(G,G);r_{--}^2} &= 1, \quad z_{r_{--},r_{--},r_{--}}^{(G,G);1_{--}} = e^{-i\frac{2\pi}{3}}, \quad z_{r_{--},r_{--},r_{--}}^{(G,G);r_{--}} = e^{i\frac{2\pi}{3}}, \\
z_{r_{--},r_{--},s_{--}}^{(G,G);rs_{--}} &= 1, \quad z_{r_{--},r_{--},rs_{--}}^{(G,G);sr_{--}} = e^{i\frac{2\pi}{3}}, \quad z_{r_{--},r_{--},sr_{--}}^{(G,G);rs_{--}} = e^{-i\frac{2\pi}{3}}, \\
z_{r_{--},r_{--},s_{--}}^{(G,G);sr_{--}} &= 1, \quad z_{r_{--},r_{--},rs_{--}}^{(G,G);s_{--}} = e^{-i\frac{2\pi}{3}}, \quad z_{r_{--},r_{--},sr_{--}}^{(G,G);rs_{--}} = e^{i\frac{2\pi}{3}}, \\
z_{r_{++},r_{--},\alpha_{+-}}^{(G,G);\alpha_{+-}} &= z_{r_{++},r_{--},\alpha_{+-}}^{(G,G);\alpha_{+-}} = z_{r_{++},r_{--},\beta_{+-}}^{(G,G);\beta_{+-}} = z_{r_{++},r_{--},\beta_{+-}}^{(G,G);\beta_{+-}} = e^{i\frac{2\pi}{3}}, \\
z_{r_{--},r_{++},\alpha_{-+}}^{(G,G);\alpha_{-+}} &= z_{r_{--},r_{++},\alpha_{-+}}^{(G,G);\alpha_{-+}} = z_{r_{--},r_{++},\beta_{-+}}^{(G,G);\beta_{-+}} = z_{r_{--},r_{++},\beta_{-+}}^{(G,G);\beta_{-+}} = e^{i\frac{2\pi}{3}};
\end{aligned}$$

$$\begin{aligned}
z_{r_{++},r_{++},1_{++}}^{(H,H);r_{++}^2} &= 1, \quad z_{r_{++},r_{++},r_{++}}^{(H,H);r_{++}^2} = e^{-i\frac{2\pi}{3}}, \quad z_{r_{++},r_{++},r_{++}}^{(H,H);1_{++}} = e^{i\frac{2\pi}{3}}, \\
z_{r_{++},r_{++},1_{++}}^{(H,H);r_{++}^2} &= 1, \quad z_{r_{++},r_{++},r_{++}}^{(H,H);1_{++}} = e^{i\frac{2\pi}{3}}, \quad z_{r_{++},r_{++},r_{++}}^{(H,H);r_{++}} = e^{-i\frac{2\pi}{3}}, \\
z_{r_{++},r_{++},s_{++}}^{(H,H);rs_{++}} &= 1, \quad z_{r_{++},r_{++},rs_{++}}^{(H,H);sr_{++}} = e^{-i\frac{2\pi}{3}}, \quad z_{r_{++},r_{++},sr_{++}}^{(H,H);rs_{++}} = e^{i\frac{2\pi}{3}}, \\
z_{r_{++},r_{++},s_{++}}^{(H,H);sr_{++}} &= 1, \quad z_{r_{++},r_{++},rs_{++}}^{(H,H);s_{++}} = e^{i\frac{2\pi}{3}}, \quad z_{r_{++},r_{++},sr_{++}}^{(H,H);rs_{++}} = e^{-i\frac{2\pi}{3}}, \\
z_{r_{--},r_{--},1_{--}}^{(H,H);r_{--}^2} &= 1, \quad z_{r_{--},r_{--},r_{--}}^{(H,H);r_{--}^2} = e^{-i\frac{2\pi}{3}}, \quad z_{r_{--},r_{--},r_{--}}^{(H,H);1_{--}} = e^{i\frac{2\pi}{3}}, \\
z_{r_{--},r_{--},1_{--}}^{(H,H);r_{--}^2} &= 1, \quad z_{r_{--},r_{--},r_{--}}^{(H,H);1_{--}} = e^{i\frac{2\pi}{3}}, \quad z_{r_{--},r_{--},r_{--}}^{(H,H);r_{--}} = e^{-i\frac{2\pi}{3}}, \\
z_{r_{--},r_{--},s_{--}}^{(H,H);rs_{--}} &= 1, \quad z_{r_{--},r_{--},rs_{--}}^{(H,H);sr_{--}} = e^{-i\frac{2\pi}{3}}, \quad z_{r_{--},r_{--},sr_{--}}^{(H,H);rs_{--}} = e^{i\frac{2\pi}{3}}, \\
z_{r_{--},r_{--},s_{--}}^{(H,H);sr_{--}} &= 1, \quad z_{r_{--},r_{--},rs_{--}}^{(H,H);s_{--}} = e^{i\frac{2\pi}{3}}, \quad z_{r_{--},r_{--},sr_{--}}^{(H,H);rs_{--}} = e^{-i\frac{2\pi}{3}}, \\
z_{r_{++},r_{--},\alpha_{+-}}^{(H,H);\alpha_{+-}} &= z_{r_{++},r_{--},\alpha_{+-}}^{(H,H);\alpha_{+-}} = z_{r_{++},r_{--},\beta_{+-}}^{(H,H);\beta_{+-}} = z_{r_{++},r_{--},\beta_{+-}}^{(H,H);\beta_{+-}} = e^{-i\frac{2\pi}{3}}, \\
z_{r_{--},r_{++},\alpha_{-+}}^{(H,H);\alpha_{-+}} &= z_{r_{--},r_{++},\alpha_{-+}}^{(H,H);\alpha_{-+}} = z_{r_{--},r_{++},\beta_{-+}}^{(H,H);\beta_{-+}} = z_{r_{--},r_{++},\beta_{-+}}^{(H,H);\beta_{-+}} = e^{-i\frac{2\pi}{3}};
\end{aligned}$$

$$\begin{aligned}
z_{s_{++},s_{++},1_{++}}^{(D,D);s_{++}} &= z_{s_{++},rs_{++},r_{++}}^{(D,D);sr_{++}} = z_{s_{++},sr_{++},r_{++}}^{(D,D);rs_{++}} = 1, \\
z_{rs_{++},rs_{++},1_{++}}^{(D,D);rs_{++}} &= z_{rs_{++},sr_{++},r_{++}}^{(D,D);s_{++}} = z_{rs_{++},s_{++},r_{++}}^{(D,D);sr_{++}} = 1, \\
z_{sr_{++},sr_{++},1_{++}}^{(D,D);sr_{++}} &= z_{sr_{++},s_{++},r_{++}}^{(D,D);rs_{++}} = z_{sr_{++},rs_{++},r_{++}}^{(D,D);s_{++}} = 1, \\
z_{s_{++},s_{++},s_{++}}^{(D,D);1_{++}} &= z_{s_{++},rs_{++},sr_{++}}^{(D,D);r_{++}} = z_{s_{++},sr_{++},rs_{++}}^{(D,D);r_{++}} = 1, \\
z_{rs_{++},rs_{++},rs_{++}}^{(D,D);1_{++}} &= z_{rs_{++},sr_{++},s_{++}}^{(D,D);r_{++}} = z_{rs_{++},s_{++},sr_{++}}^{(D,D);r_{++}} = 1, \\
z_{sr_{++},sr_{++},sr_{++}}^{(D,D);1_{++}} &= z_{sr_{++},s_{++},sr_{++}}^{(D,D);r_{++}} = z_{sr_{++},rs_{++},s_{++}}^{(D,D);r_{++}} = 1,
\end{aligned}$$

$$\begin{aligned}
z_{s_{--},s_{--},1_{--}}^{(D,D);s_{--}} &= z_{s_{--},rs_{--},r_{--}}^{(D,D);sr_{--}} = z_{s_{--},sr_{--},r_{--}^2}^{(D,D);rs_{--}} = 1, \\
z_{rs_{--},rs_{--},1_{--}}^{(D,D);rs_{--}} &= z_{rs_{--},sr_{--},r_{--}}^{(D,D);s_{--}} = z_{rs_{--},s_{--},r_{--}^2}^{(D,D);sr_{--}} = 1, \\
z_{sr_{--},sr_{--},1_{--}}^{(D,D);sr_{--}} &= z_{sr_{--},s_{--},r_{--}}^{(D,D);rs_{--}} = z_{sr_{--},rs_{--},r_{--}^2}^{(D,D);s_{--}} = 1, \\
z_{s_{--},s_{--},s_{--}}^{(D,D);1_{--}} &= z_{s_{--},rs_{--},sr_{--}}^{(D,D);r_{--}} = z_{s_{--},sr_{--},rs_{--}}^{(D,D);r_{--}^2} = 1, \\
z_{rs_{--},rs_{--},rs_{--}}^{(D,D);1_{--}} &= z_{rs_{--},sr_{--},s_{--}}^{(D,D);r_{--}} = z_{rs_{--},s_{--},sr_{--}}^{(D,D);r_{--}^2} = 1, \\
z_{sr_{--},sr_{--},sr_{--}}^{(D,D);1_{--}} &= z_{sr_{--},s_{--},sr_{--}}^{(D,D);R} = z_{sr_{--},rs_{--},s_{--}}^{(D,D);r_{--}^2} = 1, \\
z_{s_{++},s_{--},\alpha_{+-}}^{(D,D);\beta_{+-}} &= z_{s_{++},rs_{--},\alpha_{+-}}^{(D,D);\beta_{+-}} = z_{s_{++},s_{--},\alpha_{+-}}^{(D,D);\beta_{+-}} = z_{s_{++},sr_{--},\alpha_{+-}}^{(D,D);\beta_{+-}} = z_{sr_{++},s_{--},\alpha_{+-}}^{(D,D);\beta_{+-}} = \frac{1}{\sqrt{3}}, \\
z_{rs_{++},rs_{--},\alpha_{+-}}^{(D,D);\beta_{+-}} &= z_{sr_{++},sr_{--},\alpha_{+-}}^{(D,D);\beta_{+-}} = \frac{e^{i\frac{2\pi}{3}}}{\sqrt{3}}, \quad z_{rs_{++},sr_{--},\alpha_{+-}}^{(D,D);\beta_{+-}} = z_{sr_{++},rs_{--},\alpha_{+-}}^{(D,D);\beta_{+-}} = \frac{e^{-i\frac{2\pi}{3}}}{\sqrt{3}}, \\
z_{s_{++},s_{--},\beta_{+-}}^{(D,D);\alpha_{+-}} &= z_{s_{++},rs_{--},\beta_{+-}}^{(D,D);\alpha_{+-}} = z_{rs_{++},s_{--},\beta_{+-}}^{(D,D);\alpha_{+-}} = z_{s_{++},sr_{--},\beta_{+-}}^{(D,D);\alpha_{+-}} = z_{sr_{++},s_{--},\beta_{+-}}^{(D,D);\alpha_{+-}} = \frac{1}{\sqrt{3}}, \\
z_{rs_{++},rs_{--},\beta_{+-}}^{(D,D);\alpha_{+-}} &= z_{sr_{++},sr_{--},\beta_{+-}}^{(D,D);\alpha_{+-}} = \frac{e^{-i\frac{2\pi}{3}}}{\sqrt{3}}, \quad z_{rs_{++},sr_{--},\beta_{+-}}^{(D,D);\alpha_{+-}} = z_{sr_{++},rs_{--},\beta_{+-}}^{(D,D);\alpha_{+-}} = \frac{e^{i\frac{2\pi}{3}}}{\sqrt{3}}, \\
z_{s_{--},s_{++},\alpha_{+-}}^{(D,D);\beta_{+-}} &= z_{s_{--},rs_{++},\alpha_{+-}}^{(D,D);\beta_{+-}} = z_{rs_{--},s_{++},\alpha_{+-}}^{(D,D);\beta_{+-}} = z_{s_{--},sr_{++},\alpha_{+-}}^{(D,D);\beta_{+-}} = z_{sr_{--},s_{++},\alpha_{+-}}^{(D,D);\beta_{+-}} = \frac{1}{\sqrt{3}}, \\
z_{rs_{--},rs_{++},\alpha_{+-}}^{(D,D);\beta_{+-}} &= z_{sr_{--},sr_{++},\alpha_{+-}}^{(D,D);\beta_{+-}} = \frac{e^{i\frac{2\pi}{3}}}{\sqrt{3}}, \quad z_{rs_{--},sr_{++},\alpha_{+-}}^{(D,D);\beta_{+-}} = z_{sr_{--},rs_{++},\alpha_{+-}}^{(D,D);\beta_{+-}} = \frac{e^{-i\frac{2\pi}{3}}}{\sqrt{3}}, \\
z_{s_{--},s_{++},\beta_{+-}}^{(D,D);\alpha_{+-}} &= z_{s_{--},rs_{++},\beta_{+-}}^{(D,D);\alpha_{+-}} = z_{rs_{--},s_{++},\beta_{+-}}^{(D,D);\alpha_{+-}} = z_{s_{--},sr_{++},\beta_{+-}}^{(D,D);\alpha_{+-}} = z_{sr_{--},s_{++},\beta_{+-}}^{(D,D);\alpha_{+-}} = \frac{1}{\sqrt{3}}, \\
z_{rs_{--},rs_{++},\beta_{+-}}^{(D,D);\alpha_{+-}} &= z_{sr_{--},sr_{++},\beta_{+-}}^{(D,D);\alpha_{+-}} = \frac{e^{-i\frac{2\pi}{3}}}{\sqrt{3}}, \quad z_{rs_{--},sr_{++},\beta_{+-}}^{(D,D);\alpha_{+-}} = z_{sr_{--},rs_{++},\beta_{+-}}^{(D,D);\alpha_{+-}} = \frac{e^{i\frac{2\pi}{3}}}{\sqrt{3}};
\end{aligned}$$

$$\begin{aligned}
z_{s_{++},s_{++},1_{++}}^{(E,E);s_{++}} &= z_{s_{++},rs_{++},r_{++}}^{(E,E);sr_{++}} = z_{s_{++},sr_{++},r_{++}^2}^{(E,E);rs_{++}} = 1, \\
z_{rs_{++},rs_{++},1_{++}}^{(E,E);rs_{++}} &= z_{rs_{++},sr_{++},r_{++}}^{(E,E);s_{++}} = z_{rs_{++},s_{++},r_{++}^2}^{(E,E);sr_{++}} = 1, \\
z_{sr_{++},sr_{++},1_{++}}^{(E,E);sr_{++}} &= z_{sr_{++},s_{++},r_{++}}^{(E,E);rs_{++}} = z_{sr_{++},rs_{++},r_{++}^2}^{(E,E);s_{++}} = 1, \\
z_{s_{++},s_{++},s_{++}}^{(E,E);1_{++}} &= z_{s_{++},rs_{++},sr_{++}}^{(E,E);r_{++}} = z_{s_{++},sr_{++},rs_{++}}^{(E,E);r_{++}^2} = -1, \\
z_{rs_{++},rs_{++},rs_{++}}^{(E,E);1_{++}} &= z_{rs_{++},sr_{++},s_{++}}^{(E,E);r_{++}} = z_{rs_{++},s_{++},sr_{++}}^{(E,E);r_{++}^2} = -1, \\
z_{sr_{++},sr_{++},sr_{++}}^{(E,E);1_{++}} &= z_{sr_{++},s_{++},sr_{++}}^{(E,E);r_{++}} = z_{sr_{++},rs_{++},s_{++}}^{(E,E);r_{++}^2} = -1, \\
z_{s_{--},s_{--},1_{--}}^{(E,E);s_{--}} &= z_{s_{--},rs_{--},r_{--}}^{(E,E);sr_{--}} = z_{s_{--},sr_{--},r_{--}^2}^{(E,E);rs_{--}} = 1, \\
z_{rs_{--},rs_{--},1_{--}}^{(E,E);rs_{--}} &= z_{rs_{--},sr_{--},r_{--}}^{(E,E);s_{--}} = z_{rs_{--},s_{--},r_{--}^2}^{(E,E);sr_{--}} = 1, \\
z_{sr_{--},sr_{--},1_{--}}^{(E,E);sr_{--}} &= z_{sr_{--},s_{--},r_{--}}^{(E,E);rs_{--}} = z_{sr_{--},rs_{--},r_{--}^2}^{(E,E);s_{--}} = 1, \\
z_{s_{--},s_{--},s_{--}}^{(E,E);1_{--}} &= z_{s_{--},rs_{--},sr_{--}}^{(E,E);r_{--}} = z_{s_{--},sr_{--},rs_{--}}^{(E,E);r_{--}^2} = -1,
\end{aligned}$$

$$\begin{aligned}
z_{rs_{--},rs_{--},rs_{--}}^{(E,E);1_{--}} &= z_{rs_{--},sr_{--},s_{--}}^{(E,E);r_{--}} = z_{rs_{--},s_{--},sr_{--}}^{(E,E);r_{--}^2} = -1, \\
z_{sr_{--},sr_{--},sr_{--}}^{(E,E);1_{--}} &= z_{sr_{--},s_{--},sr_{--}}^{(E,E);R} = z_{sr_{--},rs_{--},s_{--}}^{(E,E);r_{--}^2} = -1, \\
z_{s_{++},s_{--},\alpha_{+-}}^{(E,E);\beta_{+-}} &= z_{s_{++},rs_{--},\alpha_{+-}}^{(E,E);\beta_{+-}} = z_{rs_{++},s_{--},\alpha_{+-}}^{(E,E);\beta_{+-}} = z_{s_{++},sr_{--},\alpha_{+-}}^{(E,E);\beta_{+-}} = z_{sr_{++},s_{--},\alpha_{+-}}^{(E,E);\beta_{+-}} = \frac{1}{\sqrt{3}}, \\
z_{rs_{++},rs_{--},\alpha_{+-}}^{(E,E);\beta_{+-}} &= z_{sr_{++},sr_{--},\alpha_{+-}}^{(E,E);\beta_{+-}} = \frac{e^{i\frac{2\pi}{3}}}{\sqrt{3}}, \quad z_{rs_{++},sr_{--},\alpha_{+-}}^{(E,E);\beta_{+-}} = z_{sr_{++},rs_{--},\alpha_{+-}}^{(E,E);\beta_{+-}} = \frac{e^{-i\frac{2\pi}{3}}}{\sqrt{3}}, \\
z_{s_{++},s_{--},\beta_{+-}}^{(E,E);\alpha_{+-}} &= z_{s_{++},rs_{--},\beta_{+-}}^{(E,E);\alpha_{+-}} = z_{rs_{++},s_{--},\beta_{+-}}^{(E,E);\alpha_{+-}} = z_{s_{++},sr_{--},\beta_{+-}}^{(E,E);\alpha_{+-}} = z_{sr_{++},s_{--},\beta_{+-}}^{(E,E);\alpha_{+-}} = \frac{1}{\sqrt{3}}, \\
z_{rs_{++},rs_{--},\beta_{+-}}^{(E,E);\alpha_{+-}} &= z_{sr_{++},sr_{--},\beta_{+-}}^{(E,E);\alpha_{+-}} = \frac{e^{-i\frac{2\pi}{3}}}{\sqrt{3}}, \quad z_{rs_{++},sr_{--},\beta_{+-}}^{(E,E);\alpha_{+-}} = z_{sr_{++},rs_{--},\beta_{+-}}^{(E,E);\alpha_{+-}} = \frac{e^{i\frac{2\pi}{3}}}{\sqrt{3}}, \\
z_{s_{--},s_{++},\alpha_{-+}}^{(E,E);\beta_{-+}} &= z_{s_{--},rs_{++},\alpha_{-+}}^{(E,E);\beta_{-+}} = z_{rs_{--},s_{++},\alpha_{-+}}^{(E,E);\beta_{-+}} = z_{s_{--},sr_{++},\alpha_{-+}}^{(E,E);\beta_{-+}} = z_{sr_{--},s_{++},\alpha_{-+}}^{(E,E);\beta_{-+}} = \frac{1}{\sqrt{3}}, \\
z_{rs_{--},rs_{++},\alpha_{-+}}^{(E,E);\beta_{-+}} &= z_{sr_{--},sr_{++},\alpha_{-+}}^{(E,E);\beta_{-+}} = \frac{e^{i\frac{2\pi}{3}}}{\sqrt{3}}, \quad z_{rs_{--},sr_{++},\alpha_{-+}}^{(E,E);\beta_{-+}} = z_{sr_{--},rs_{++},\alpha_{-+}}^{(E,E);\beta_{-+}} = \frac{e^{-i\frac{2\pi}{3}}}{\sqrt{3}}, \\
z_{s_{--},s_{++},\beta_{-+}}^{(E,E);\alpha_{-+}} &= z_{s_{--},rs_{++},\beta_{-+}}^{(E,E);\alpha_{-+}} = z_{rs_{--},s_{++},\beta_{-+}}^{(E,E);\alpha_{-+}} = z_{s_{--},sr_{++},\beta_{-+}}^{(E,E);\alpha_{-+}} = z_{sr_{--},s_{++},\beta_{-+}}^{(E,E);\alpha_{-+}} = \frac{1}{\sqrt{3}}, \\
z_{rs_{--},rs_{++},\beta_{-+}}^{(E,E);\alpha_{-+}} &= z_{sr_{--},sr_{++},\beta_{-+}}^{(E,E);\alpha_{-+}} = \frac{e^{-i\frac{2\pi}{3}}}{\sqrt{3}}, \quad z_{rs_{--},sr_{++},\beta_{-+}}^{(E,E);\alpha_{-+}} = z_{sr_{--},rs_{++},\beta_{-+}}^{(E,E);\alpha_{-+}} = \frac{e^{i\frac{2\pi}{3}}}{\sqrt{3}}.
\end{aligned}$$

F Anyon Fragmentation Pattern

In this section, we provide the non-Abelian anyon fragmentation pattern of $D(S_3)$ phase under EM-exchange symmetry (in α -gauge), as shown in Table 3.

G Proof that ρ^G and ρ^H are not projective representations

Here, we prove that the representations ρ^G (4.5) and ρ^H (4.6) are not projective representations, which are equivalent to linear representations of \mathbb{Z}_2 , although they appear to be. Our proof goes by showing that the phase factors in (4.5) and (4.6), which are due to the nonlinearity indicator ω , cannot be transformed away consistently:

Since the nonlinearity indicator ω only depends on the Pachner moves, we can express the components of ω solely using $6j$ -symbols⁵ as

$$\begin{aligned}
\omega_{r,r} &= 3G_{r,\alpha,\alpha}^{r^2,\alpha,\alpha} G_{\alpha,\alpha,\alpha}^{1,r,r^2} G_{\alpha,\alpha,\alpha}^{1,r,r^2}, \\
\omega_{r^2,r^2} &= 3G_{r^2,\alpha,\alpha}^{r,\alpha,\alpha} G_{\alpha,\alpha,\alpha}^{1,r,r^2} G_{\alpha,\alpha,\alpha}^{1,r,r^2}, \\
\omega_{r,r^2} &= 3G_{r^2,\alpha,\alpha}^{r^2,\alpha,\alpha} G_{\alpha,\alpha,\alpha}^{1,r,r^2} G_{\alpha,\alpha,\alpha}^{1,r,r^2}, \\
\omega_{r^2,r} &= 3G_{r,\alpha,\alpha}^{r,\alpha,\alpha} G_{\alpha,\alpha,\alpha}^{1,r,r^2} G_{\alpha,\alpha,\alpha}^{1,r,r^2}.
\end{aligned} \tag{G.1}$$

⁵ As $G_{c_{kl}d_{ij}f_{jk}e_{ik}}^{a_{ij}b_{jk}e_{ik}} = G_{c_{\bar{k}\bar{l}}d_{\bar{i}\bar{j}}f_{\bar{j}\bar{k}}e_{\bar{i}\bar{k}}}^{a_{\bar{i}\bar{j}}b_{\bar{j}\bar{k}}e_{\bar{i}\bar{k}}}$ always holds for any $i, j, k, l \in \{+, -\}$ due to the symmetry, we use G_{cdf}^{abe} to denote them for convenience:

$$G_{cdf}^{abe} := G_{c_{kl}d_{ij}f_{jk}e_{ik}}^{a_{ij}b_{jk}e_{ik}} = G_{c_{\bar{k}\bar{l}}d_{\bar{i}\bar{j}}f_{\bar{j}\bar{k}}e_{\bar{i}\bar{k}}}^{a_{\bar{i}\bar{j}}b_{\bar{j}\bar{k}}e_{\bar{i}\bar{k}}}.$$

Non-Abelian anyons	Definite symmetry charge states (spaces)	Symmetry charge
$C \oplus F$	$\text{span}\{C_{1_1} + F_r, C_{1_2} + F_{r^2}\}$	0
	$\text{span}\{C_{1_1} - F_r, C_{1_2} - F_{r^2}\}$	$\frac{1}{2}$
G	$\text{span}\{G_r, G_{r^2}\}$	$\frac{1}{3}$
H	$H_r + H_{r^2}$	$\frac{2}{3}$
	$H_r - H_{r^2}$	$\frac{1}{6}$
D	$D_{rs} - D_{sr}$	$\frac{1}{4}$
	$(1 + \sqrt{3})D_s + D_{rs} + D_{sr}$	0
	$(1 - \sqrt{3})D_s + D_{rs} + D_{sr}$	$\frac{1}{2}$
E	$E_{rs} - E_{sr}$	$\frac{1}{4}$
	$(1 + \sqrt{3})E_s + E_{rs} + E_{sr}$	0
	$(1 - \sqrt{3})E_s + E_{rs} + E_{sr}$	$\frac{1}{2}$

Table 3: Non-Abelian anyon fragmentation pattern of $D(S_3)$ phase under EM-exchange symmetry (in α -gauge)

In order to transform them away, we can only resort to the gauge transformation on the $6j$ -symbols[9, 47]

$$G_{cdf}^{abe} \rightarrow \frac{u_{abe}u_{cde^*}}{u_{daf^*}u_{bcf}} G_{cdf}^{abe}. \quad (\text{G.2})$$

But this is impossible without violating the gauge constraint condition

$$G_{i,\alpha,\alpha}^{0,\alpha,\alpha} = 1, \quad \forall i \in \{1, r, r^2\}, \quad (\text{G.3})$$

which must be satisfied by the string-net model with any input UFC.

Thus, the phase factors in (4.5) (4.6) cannot be transformed away consistently in the string-net model, rendering ρ^G and ρ^H truly nonlinear representations.

References

- [1] T. Lan and X. G. Wen, *Physical Review B - Condensed Matter and Materials Physics* **90**, 115119 (2014), arXiv:1311.1784 .
- [2] Y. Hu, N. Geer, and Y.-S. Wu, *Physical Review B* **97**, 195154 (2018), arXiv:1502.03433 .
- [3] H. Wang, Y. Li, Y. Hu, and Y. Wan, *Journal of High Energy Physics* **2020**, 30 (2020).
- [4] Y. Zhao, S. Huang, H. Wang, Y. Hu, and Y. Wan, *SciPost Physics Core* **6**, 076 (2023).
- [5] Y. Zhao, H. Wang, Y. Hu, and Y. Wan, *Journal of High Energy Physics* **2024**, 1 (2024).
- [6] Y. Zhao and Y. Wan, arXiv preprint arXiv:2408.02664 (2024).
- [7] Y. Zhao and Y. Wan, arXiv preprint arXiv:2409.05852 (2024).

- [8] Y. Zhao and Y. Wan, arXiv preprint arXiv:2506.05319 (2025).
- [9] N. Fu, Y. Zhao, and Y. Wan, “Symmetry-enriched topological orders and their gauging: A string-net model realization,” (2025), companion paper, to appear in arXiv soon.
- [10] A. Mesaros and Y. Ran, *Physical Review B* **87**, 155115 (2013), arXiv:1212.0835 .
- [11] L.-Y. Hung and Y. Wan, *International Journal of Modern Physics B* **28**, 1450172 (2014).
- [12] L.-Y. Hung and Y. Wan, *Physical Review B* **87**, 195103 (2013).
- [13] Y.-M. Lu and A. Vishwanath, *Physical Review B* **93**, 155121 (2016).
- [14] Y. Gu, L.-Y. Hung, and Y. Wan, *Phys. Rev. B* **90**, 245125 (2014), arXiv:1402.3356 .
- [15] M. Barkeshli, P. Bonderson, M. Cheng, and Z. Wang, *Physical Review B* **100**, 115147 (2019), arXiv:1410.4540 .
- [16] L. Chang, M. Cheng, S. X. Cui, Y. Hu, W. Jin, R. Movassagh, P. Naaijken, Z. Wang, and A. Young, *Journal of Physics A: Mathematical and Theoretical* **48**, 12FT01 (2015).
- [17] C. Heinrich, F. Burnell, L. Fidkowski, and M. Levin, *Physical Review B* **94**, 235136 (2016).
- [18] M. Cheng, Z.-C. Gu, S. Jiang, and Y. Qi, *Physical Review B* **96**, 115107 (2017).
- [19] D. J. Williamson and Z. Wang, *Annals of Physics* **377**, 311 (2017).
- [20] D. J. Williamson, N. Bultinck, and F. Verstraete, arXiv preprint arXiv:1711.07982 (2017).
- [21] S.-Q. Ning, Z.-X. Liu, and P. Ye, (2018), arXiv:1801.01638 .
- [22] Y. Hu, Z. Huang, L.-Y. Hung, and Y. Wan, *Journal of High Energy Physics* **2022**, 26 (2022).
- [23] Q.-R. Wang and M. Cheng, *Physical Review B* **106**, 115104 (2022).
- [24] M. A. Levin and X.-G. Wen, *Physical Review B—Condensed Matter and Materials Physics* **71**, 045110 (2005).
- [25] X. Chen, F. Wang, Y.-M. Lu, and D.-H. Lee, *Nuclear Physics B* **873**, 248 (2013).
- [26] J. C. Wang, Z.-C. Gu, and X.-G. Wen, *Physical review letters* **114**, 031601 (2015).
- [27] D. J. Williamson, N. Bultinck, and F. Verstraete, arXiv:1711.07982v1 .
- [28] L.-Y. Hung and X.-g. Wen, *Physical Review B* **87**, 165107 (2013), arXiv:1212.1827v1 .
- [29] J. Y. Lee, A. M. Turner, and A. Vishwanath, *Physical Review B* **98**, 214416 (2018).
- [30] H. Yao, L. Fu, and X.-L. Qi, arXiv preprint arXiv:1012.4470 (2010).
- [31] A. Essin and M. Hermele, *Phys. Rev. B* **87**, 104406 (2013) (2012), arXiv:1212.0593v2 .
- [32] M. Barkeshli, E. Berg, and S. Kivelson, *Science* **346**, 722 (2014).
- [33] M. Barkeshli, P. Bonderson, M. Cheng, and Z. Wang, *Physical Review B* **100**, 115147 (2019).
- [34] H. Song and M. Hermele, *Physical Review B* **91**, 014405 (2015).
- [35] Y. Li and M. Litvinov, arXiv preprint arXiv:2405.15951 (2024).
- [36] S. D. Sarma, M. Freedman, and C. Nayak, *npj Quantum Information* **2015 1:1 1**, 1 (2015), arXiv:1501.02813 .
- [37] A. Stern, “Anyons and the quantum Hall effect-A pedagogical review,” (2008), arXiv:0711.4697 .

- [38] L. Kong and Z.-H. Zhang, “An invitation to topological orders and category theory,” (2022), [arXiv:2205.05565 \[cond-mat.str-el\]](#) .
- [39] C. F. B. Lo, A. Lyons, R. Verresen, A. Vishwanath, and N. Tantivasadakarn, arXiv preprint [arXiv:2502.14974](#) (2025).
- [40] K. Iguchi, [Physical Review Letters](#) **78**, 3233 (1997).
- [41] S. Guruswamy and K. Schoutens, [Nuclear Physics B](#) **556**, 530 (1999), [arXiv:9903045 \[cond-mat\]](#) .
- [42] M. Barkeshli, C.-M. Jian, and X.-L. Qi, [Physical Review B](#) **87**, 045130 (2013).
- [43] Y. Hu, S. D. Stirling, and Y. S. Wu, [Physical Review B](#) **89**, 115133 (2014), [arXiv:1303.1586](#) .
- [44] Y. Li, H. Wang, Y. Hu, and Y. Wan, [Journal of High Energy Physics](#) **2019**, 1 (2019).
- [45] Y. Li, H. Wang, Y. Hu, and Y. Wan, [Journal of High Energy Physics](#) **2019**, 78 (2019).
- [46] Y. Hu, S. D. Stirling, and Y.-S. Wu, [Physical Review B—Condensed Matter and Materials Physics](#) **85**, 075107 (2012).
- [47] L.-Y. Hung and Y. Wan, [Physical Review B](#) **86**, 235132 (2012), [arXiv:1207.6169](#) .